

EFFECT OF THERMOMECHANICAL TREATMENT
ON THE MICROSTRUCTURE AND MECHANICAL
PROPERTIES OF AISI 52100 STEEL

Clarence W. Schultz

NAVAL POSTGRADUATE SCHOOL

Monterey, California



THESIS

EFFECT OF THERMOMECHANICAL TREATMENT
ON THE MICROSTRUCTURE AND MECHANICAL
PROPERTIES OF AISI 52100 STEEL

by

Clarence W. Schultz

June 1981

Thesis Advisor:

T.R. McNelley

Approved for public release; distribution unlimited

T200667

Unclassified

SECURITY CLASSIFICATION OF THIS PAGE (When Data Entered)

REPORT DOCUMENTATION PAGE		READ INSTRUCTIONS BEFORE COMPLETING FORM
1. REPORT NUMBER	2. GOVT ACCESSION NO.	3. RECIPIENT'S CATALOG NUMBER
4. TITLE (and Subtitle) Effect of Thermomechanical Treatment on the Microstructure and Mechanical Properties of AISI 52100 Steel		5. TYPE OF REPORT & PERIOD COVERED Master's Thesis June 1981
7. AUTHOR(s) Clarence W. Schultz		6. PERFORMING ORG. REPORT NUMBER
9. PERFORMING ORGANIZATION NAME AND ADDRESS Naval Postgraduate School Monterey, California 93940		8. CONTRACT OR GRANT NUMBER(s)
11. CONTROLLING OFFICE NAME AND ADDRESS Naval Postgraduate School Monterey, California 93940		10. PROGRAM ELEMENT, PROJECT, TASK AREA & WORK UNIT NUMBERS
14. MONITORING AGENCY NAME & ADDRESS (if different from Controlling Office)		12. REPORT DATE June 1981
		13. NUMBER OF PAGES 102
		15. SECURITY CLASS. (of this report) Unclassified
		15a. DECLASSIFICATION/DOWNGRADING SCHEDULE
16. DISTRIBUTION STATEMENT (of this Report) Approved for public release; distribution unlimited.		
17. DISTRIBUTION STATEMENT (of the abstract entered in Block 20, if different from Report)		
18. SUPPLEMENTARY NOTES		
19. KEY WORDS (Continue on reverse side if necessary and identify by block number) 52100 Steel, thermomechanical processing; heat treatment; microstructure; microstructural refinement; grain size, carbide particle size; retained austenite; mechanical properties; hardness		
20. ABSTRACT (Continue on reverse side if necessary and identify by block number) The effects of various thermo-mechanical treatments on the microstructure and mechanical properties of AISI 52100 steel have been investigated using a combination of optical and transmission electron microscopy in conjunction with standard mechanical testing. The response of the as-treated material to various hardening and tempering treatments has been determined and compared to that of material processed using a standard commercial technique. The results indicate that the thermo-mechanical treatments examined refine the microstructure and increase the tensile strength of AISI 52100 steel.		

DD FORM 1 JAN 73 1473

EDITION OF 1 NOV 65 IS OBSOLETE
S/N 0102-014-6601

Unclassified

SECURITY CLASSIFICATION OF THIS PAGE (When Data Entered)

Article 20 continued:

ing these treatments allows processing of the steel to be accomplished at lower austenitizing temperatures and in shorter times than in currently utilized techniques. Additionally, the degradation of mechanical properties by time at various tempering temperatures is reduced.

Effect of Thermomechanical Treatment
on the Microstructure and Mechanical
Properties of AISI 52100 Steel

by

Clarence W. Schultz
Lieutenant, United States Navy
B.S.M.E., University of Texas, 1974

Submitted in partial fulfillment of the
requirements for the degree of

MASTER OF SCIENCE IN MECHANICAL ENGINEERING

from the

NAVAL POSTGRADUATE SCHOOL
June 1981

ABSTRACT

The effects of various thermo-mechanical treatments on the microstructure and mechanical properties of AISI 52100 steel have been investigated using a combination of optical and transmission electron microscopy in conjunction with standard mechanical testing. The response of the as-treated material to various hardening and tempering treatments has been determined and compared to that of material processed using a standard commercial technique.

The results indicate that the thermo-mechanical treatments examined refine the microstructure and increase the tensile strength of AISI 52100 steel. Using these treatments allows processing of the steel to be accomplished at lower austenitizing temperatures and in shorter times than in currently utilized techniques. Additionally, the degradation of mechanical properties by time at various tempering temperatures is reduced.

TABLE OF CONTENTS

I.	INTRODUCTION AND BACKGROUND -----	12
A.	INTRODUCTION -----	12
B.	WARM-ROLLING AND SUPERPLASTICITY -----	14
C.	PROPERTIES AND HEAT TREATMENT OF AISI 52100 STEEL -----	21
II.	MATERIAL PROCESSING AND EXPERIMENTAL PROCEDURE ---	27
A.	MATERIAL PROCESSING -----	27
B.	EXPERIMENTAL PROCEDURE -----	34
	1. Hardening Response -----	34
	2. Tempering Response -----	35
	3. Optical Microscopy -----	36
	4. Transmission Electron Microscopy -----	37
III.	RESULTS AND DISCUSSION -----	39
A.	EFFECT OF PRE-ROLLING TREATMENTS AND OF ROLLING -----	39
	1. Mechanical Test Results -----	39
	2. Optical Microscopy Results -----	40
	3. Transmission Electron Microscopy Results -	48
	4. Summary of Effects -----	61
B.	HARDENING RESPONSE OF AS-TREATED MATERIAL ----	66
	1. Mechanical Test Results -----	66
	2. Microstructural Results -----	76
	3. Summary of Effects -----	85
C.	TEMPERING RESPONSE OF HARDENED MATERIAL -----	85

IV. CONCLUSIONS	-----	97
LIST OF REFERENCES	-----	98
INITIAL DISTRIBUTION LIST	-----	101

LIST OF FIGURES

Figure 1.	Iron-Carbon Equilibrium Diagram -----	13
Figure 2.	Microstructure of Normalized 1.5% Carbon Low-Alloy Steel -----	16
Figure 3.	Microstructure of As-Rolled Normalized AISI 52100 Steel -----	20
Figure 4.	Micrographs of As-Received AISI 52100 Steel -----	24
Figure 5.	Schematic of Thermo-Mechanical Treatment-B -----	29
Figure 6.	Schematic of Thermo-Mechanical Treatment-C -----	30
Figure 7.	Schematic of Thermo-Mechanical Treatment-D -----	31
Figure 8.	Schematic of Thermo-Mechanical Treatment-E -----	32
Figure 9.	Comparison of Thermo-Mechanical Treatments -----	41
Figure 10.	Microstructural Effect of Treatment-B -----	43
Figure 11.	Microstructural Effect of Treatment-C -----	44
Figure 12.	Microstructural Effect of Treatment-D -----	46
Figure 13.	Microstructural Effect of Treatment-E -----	47
Figure 14.	Carbon Extraction Micrographs of Treatment-B (as-rolled) -----	50
Figure 15a.	Transmission Electron Microscope Thin Foil Micrograph of As-Rolled Treatment-B --	51
Figure 15b.	T.E.M. Thin Foil Micrographs of As-Rolled Treatment-B -----	52
Figure 16.	Carbon Extraction Micrograph of Treatment-C (prior to rolling) -----	54

Figure 17a.	Transmission Electron Microscope Thin Foil Micrograph of Treatment-C Prior to Rolling -----	55
Figure 17b.	T.E.M. Thin Foil Micrograph of Treatment-C Prior to Rolling -----	56
Figure 18.	Carbon Extraction Micrograph of Treatment-C (as rolled) -----	57
Figure 19a.	Transmission Electron Microscope Thin Foil Micrograph of As-Rolled Treatment-C -----	59
Figure 19b.	T.E.M. Thin Foil Micrograph of As-Rolled Treatment-C -----	60
Figure 20.	Carbon Extraction Micrograph of Treatment-D (prior to rolling) -----	62
Figure 21.	Carbon Extraction Micrograph of Treatment-D (as rolled) -----	63
Figure 22.	Carbon Extraction Micrograph of Treatment-B (prior to rolling) -----	64
Figure 23.	Carbon Extraction Micrograph of Treatment-E (as rolled) -----	65
Figure 24.	Hardening Response of Treatment-A -----	67
Figure 25.	Hardening Response of Treatment-B -----	68
Figure 26.	Hardening Response of Treatment-C -----	69
Figure 27.	Hardening Response to Treatment-D -----	70
Figure 28.	Hardening Response to Treatment-E -----	71
Figures 29, a and b	Optical Micrographs of Hardened AISI 52100 Steel -----	74
Figure 29c.	Optical Micrographs of Hardened AISI 52100 Steel -----	75
Figure 30.	Carbon Extraction Replica of Treatment-A Austenitized at 825 degrees Celsius -----	77
Figure 31.	Carbon Extraction Replica of Treatment-A Austenitized at 850 degrees Celsius -----	78

Figure 32.	Carbon Extraction Replica of Treatment-B Austenitized at 825 degrees Celsius -----	79
Figure 33.	Carbon Extraction Replica of Treatment-B Austenitized at 850 degrees Celsius -----	80
Figure 34.	Carbon Extraction Replica of Treatment-C Austenitized at 825 degrees Celsius -----	81
Figure 35.	Carbon Extraction Replica of Treatment-C Austenitized at 850 degrees Celsius -----	82
Figure 36.	Tempering Response of Treatment-A (Hardness) -----	87
Figure 37.	Tempering Response of Treatment-A (Tensile Strength) -----	88
Figure 38.	Tempering Response of Treatment-B (Hardness) -----	89
Figure 39.	Tempering Response of Treatment-B (Tensile Strength) -----	90
Figure 40.	Tempering Response of Treatment-C (Hardness) -----	91
Figure 41.	Tempering Response of Treatment-C (Tensile Strength) -----	92
Figure 42.	Tempering Response of Treatment-D (Hardness) -----	93
Figure 43.	Tempering Response of Treatment-D (Tensile Strength) -----	94
Figure 44.	Tempering Response of Treatment-E (Hardness) -----	95
Figure 45.	Tempering Response of Treatment-E (Tensile Strength) -----	96

LIST OF TABLES

Table 1.	Material Chemistry -----	28
Table 2.	Thermo-Mechanical Treatment Mechanical Test Data -----	40
Table 3.	Retained Austenite Determination -----	73

ACKNOWLEDGEMENT

I wish to express my deep gratitude to Professor Michael Edwards, Professor Donald Boone, and Professor Terry McNelley for their guidance and assistance, Mr. Howard Bensch and Mr. Tom Christian for their assistance, and to Professor J. P. Stark who first introduced me to the field of Material Science. I would also like to thank the staff of the Physics Department, Royal Military College of Science, for the retained austenite X-ray measurements, and to Mr. A. Doig and Mr. R. England of the Metallurgy Branch, Royal Military College of Science, for the carbide extraction replica technique. In addition, I wish to express my deepest gratitude and undying love to my wife, Patsy, and our daughters, Regina, Edee, and Chrystie without whose continuous support and patience this work would not have been possible.

I. INTRODUCTION AND BACKGROUND

A. INTRODUCTION

Ultrahigh carbon (UHC) steels, used primarily in simple machine tools and rolling-element bearings because of their high hardness and wear resistance, historically have been regarded as being inherently brittle and exhibiting extremely poor workability. However, research conducted by Professor Oleg D. Sherby and his associates at Stanford University's Department of Material Science and Engineering, has demonstrated that these steels of greater than 1.0 weight percent carbon can be readily processed by a number of thermo-mechanical techniques [Ref. 1]. These techniques involve extensive working of the UHC steel by means of rolling and/or forging as it cools from a temperature above the A_{cm} through the austenite plus cementite region of the iron-carbon phase diagram (Fig. 1). This is followed by isothermally warm-working the steel just below the A_1 temperature. This processing results in a microstructure consisting of fine, spheroidized carbides dispersed in a very fine ferrite matrix, which exhibits high room temperature strength and good ductility.

Early research at the Naval Postgraduate School on warm worked UHC steels was conducted by Goesling [Ref. 2], and Hamilton and Rowe [Ref. 3], under the direction of Professor

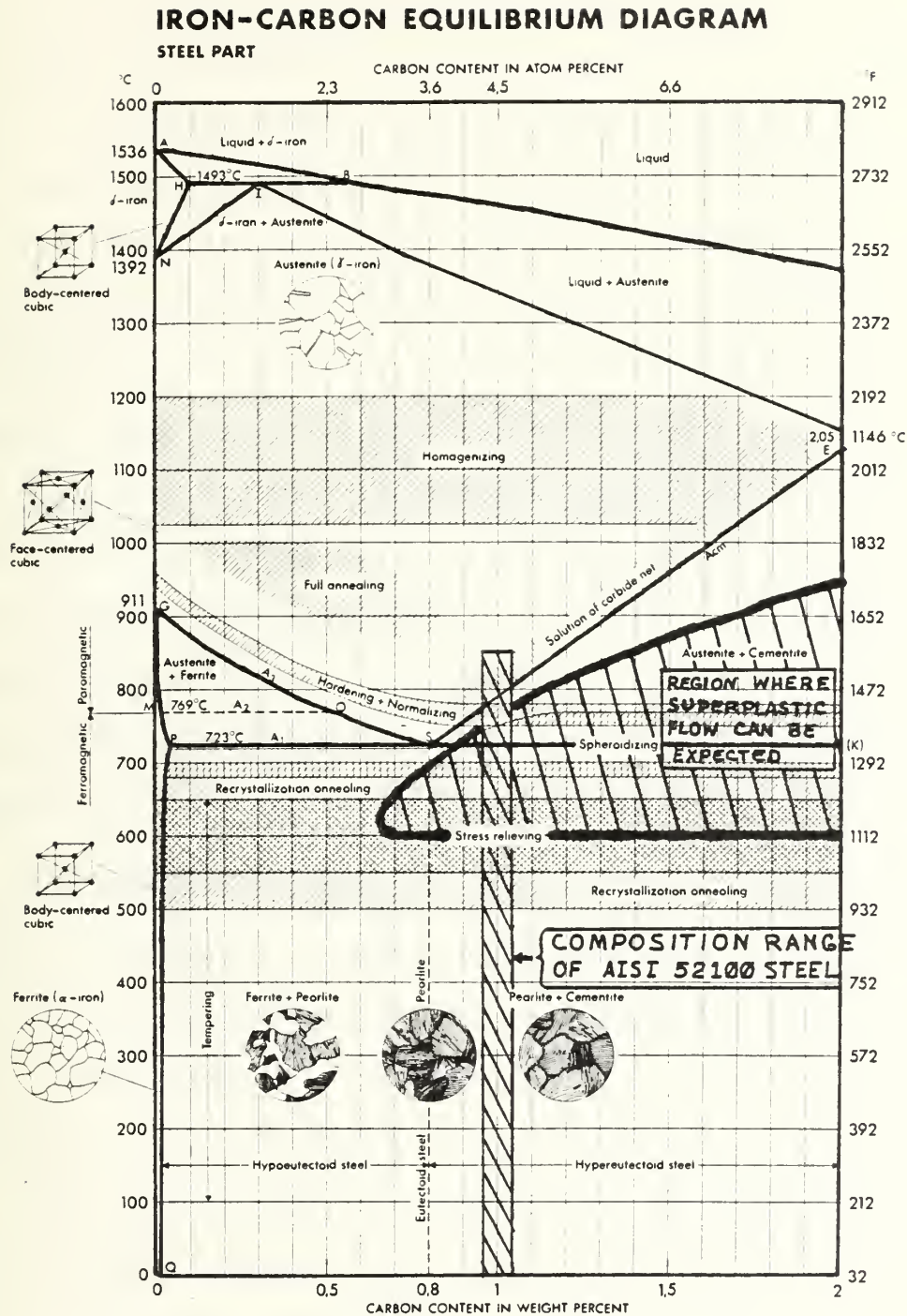


Figure 1. Iron-carbon equilibrium phase diagram showing composition range of AISI 52100 steel and the region in which superplastic behavior can be expected.

Terry R. McNelley. Their work was primarily directed towards the characterization of the mechanical, microstructural, compositional, and processing variables which effect the ballistic behavior of these steels. Their results prompted a series of examinations using commercially processed AISI 52100 steel which was normalized and then isothermally warm-rolled at various temperatures just below the A_1 , omitting the rolling of the material as it cools through the austenite plus cementite temperature range.

The current research attempts to characterize the responses of warm rolled AISI 52100 steel to various hardening and tempering treatments, and to determine the effect of various pre-rolling heat treatments on the microstructure and mechanical properties of the as-rolled and subsequently hardened and tempered material.

B. WARM-ROLLING AND SUPERPLASTICITY

Warm-rolling is a thermo-mechanical deformation process which can be utilized to refine grain structure as well as break up and refine the carbide networks found in the as-cast and normalized structures of AISI 52100 and other UHC steels. This form of processing is economically feasible in UHC steels because over the temperature range in which the deformation is performed these materials tend towards superplastic behavior.

Superplasticity, when applied to the processes of rolling and forging, refers to the greatly enhanced formability of certain materials under appropriate conditions of temperature

and strain rate [Ref.4]. In the superplastic region, large amounts of plastic deformation can be imparted to the work-piece with substantially reduced forming stresses. This behavior is always associated with: (1) a fine grain size (on the order of 1 to 10 microns); (2) deformation temperatures between 0.4 and 0.6 T_m , where T_m is the absolute melting temperature; and (3) a strain rate sensitivity factor (m) greater than 0.3 [Ref.5 and 6].

The primary microstructural characteristic necessary for superplastic flow in crystalline materials is a fine grain size at the onset of the deformation process, or development of the requisite grain structure during processing. The grain structure of normalized UHC steels consists of fairly coarse grained pearlite with significant quantities of proeutectoid cementite which forms at the prior austenite grain boundaries (Fig. 2). While this is not an ideal structure for the attainment of superplasticity, similar structures in AISI 52100 steel have been successfully warm-rolled without cracking to a true strain of -2.5, with some tendency towards superplastic behavior [Ref. 7]. In that study, Chung also demonstrated that the warm-rolling process achieved a high degree of grain refinement. This result supported earlier research conducted by Sherby [Ref. 8]. The degree of grain refinement obtained from the warm-rolling process is related to: (1) the original grain size and lamellar spacing (in the case of pearlitic structures),

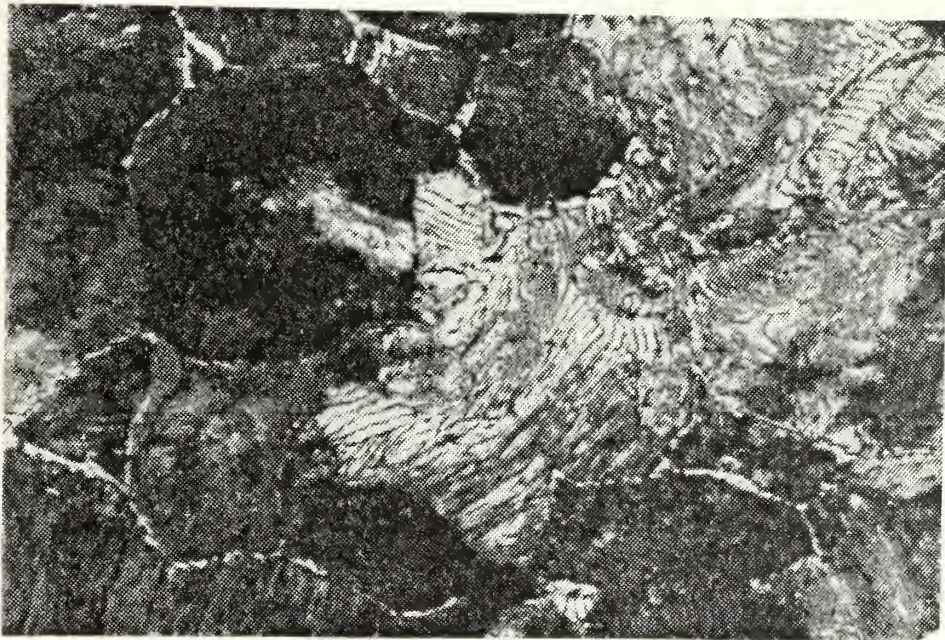


Figure 2. Microstructure of normalized 1.5% carbon low alloy steel (52100). Structure consist of coarse and fine grain pearlite, separated by massive proeutectoid cementite grain boundaries. Magnification 500X.

(2) the temperature at which the deformation is accomplished, and (3) the strain rate and total strain imparted to the material. This is directly associated with the tendency towards superplastic flow since, in addition to a fine initial grain size, superplasticity also requires a deformation temperature between 0.4 and 0.6 T_m . When applied to UHC steels this corresponds to a temperature range from approximately 450 to 775 degrees Celsius. In this temperature range Sherby has measured strain rate sensitivity factors (m) between 0.3 and 0.5 for several UHC steels [Ref. 1 and 9].

The transformation of lamellar cementite in the pearlitic structure of normalized UHC steels to spheroidite (spheroidal cementite or carbide) is a diffusion-controlled process which is greatly enhanced by concurrent plastic deformation. Early research [Ref. 10] investigating strain enhanced spheroidization in eutectoid steel (steel with 0.8 weight percent carbon) suggested that the rate controlling process is the diffusion of iron along the grain boundaries, dislocations or cementite-ferrite interfaces. It also was found that the distance between spheroidal cementite particles (interspheroidite spacing, λ) and thus the spheroidite size was a function of strain rate and temperature of the form

$$(\lambda)^n = \dot{\epsilon} \exp(Q/RT) \quad (1)$$

where n is a constant on the order of -2.0 for UHC steel, $\dot{\epsilon}$ is the strain rate, Q is the activation energy, R is the gas constant, and T is the absolute temperature. From this

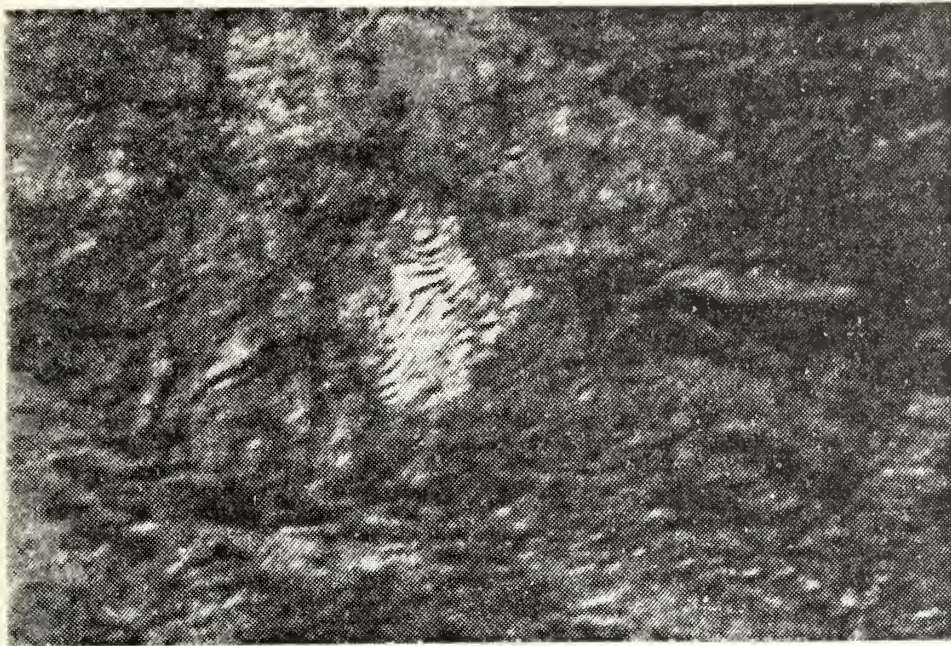
relation it can be seen that as the strain rate is increased or the temperature of deformation is decreased, the inter-particle spacing and thus the size of these second phase particles is decreased.

In UHC steels, the temperature at which the deformation is performed is restricted to approximately 85 percent of the temperature range where superplastic behavior has been observed because of the phase transformation that occurs when the material is heated above the A_1 temperature (723 degrees Celsius). When this phase transformation occurs the pearlite-cementite structure of the hypereutectoid steel, which is stable below the A_1 temperature, transforms to an austenite-cementite phase mixture. This transformation is generally reversible upon cooling.

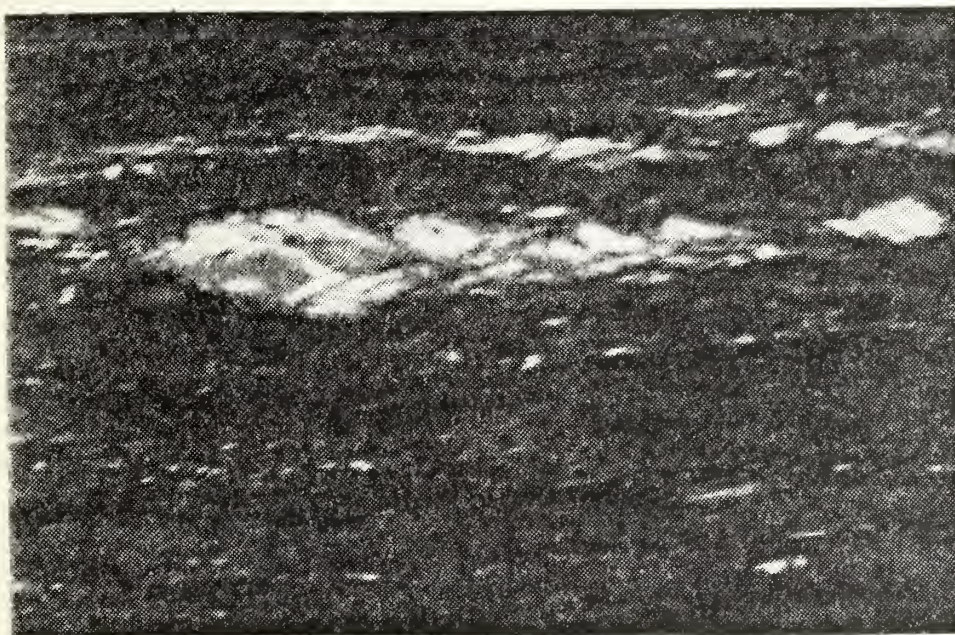
When the isothermal deformation process is carried out below the A_1 temperature, the process will tend to break up the pearlite and the proeutectoid grain boundary cementite, forming a dispersion of spheroidal cementite in a ferrite matrix. As previously noted, the interspheroidite spacing is a function of deformation temperature and the rate of deformation. However, the spheroidite tends to form at the grain boundaries. These second phase particles will pin the grain and prevent the growth that is normally associated with elevated temperature treatments just below the A_1 temperature. It also has been demonstrated by McCauley [Ref. 11] and Chung [Ref. 7], that the ability of the isothermal warm-rolling

process to break up and refine the pearlite is a function of the deformation temperature. In their work, isothermal deformation of normalized AISI 52100 steel was conducted at 550 and 650 degrees Celsius to examine the fracture toughness and fatigue properties of this material processing technique. Metallographic examination of the as-rolled structures revealed that the 650 degree treatment was far more effective in breaking up the coarse pearlitic structure (Fig. 3). However, neither treatment was completely effective in eliminating the microstructural banding resulting from the break up of the proeutectoid cementite. This suggests that the ability of the 650 degree Celsius treatment to more completely break up the pearlite, is possible due to the more rapid recrystallization at the higher deformation temperature.

In hypereutectoid or UHC steels, recrystallization occurs between 500 and 723 degrees Celsius. This nucleation and growth, diffusion-controlled process proceeds at a rate which is a function of temperature, and is enhanced by increased amounts of deformation. It has been shown that temperature and amount of deformation determines the rate at which recrystallization will occur (Ref. 12). The recrystallized grain size is independent of annealing temperature, but as the annealing temperature is increased, the driving force for grain growth after recrystallization is also increased. However, the recrystallized grain size is extremely sensitive to the amount of deformation, with the grain size decreasing



(a)



(b)

Figure 3. Microstructure of as rolled normalized AISI 52100 steel: (a) 550 degree Celsius rolling temperature; (b) 650 degree Celsius rolling temperature. Microstructures show degree of coarse pearlite break up and microstructural banding from the break up of proeutectoid grain boundary cementite. Magnification 1000X.

as the amount of total deformation increases. Further, the recrystallized grain size has been found to be highly dependent on: (1) the purity and composition of the alloy; and (2) the original grain size of the material. This is consistent with the microstructural observations of the AISI 52100 steel which was normalized and subsequently isothermally warm-rolled at 550 and 650 degrees Celsius respectively. The fine grain structure of the as rolled AISI 52100 steel was produced by heavy deformation with grain growth being restricted by the presence of the fine spheroidal carbide particles.

C. PROPERTIES AND HEAT TREATMENT OF AISI 52100 STEEL

AISI 52100 steel was developed in the 1920's for use in anti-friction bearing components [Ref. 13], where high hardness and resistance to wear and plastic deformation under localized high contact stresses are of paramount importance. These properties are associated with the development of a uniform fine tempered martensitic microstructure which is obtained by heat treatment of the hot worked alloy.

The primary requirement of early rolling-element bearing materials was high resistance to wear. High wear resistance is associated with high hardness. The hardness of a steel increases with increasing carbon content, and for a given carbon content is greatest when the structure is completely martensitic. Thus, a one weight percent carbon steel is ideally suited since hardness values between 65 and 69

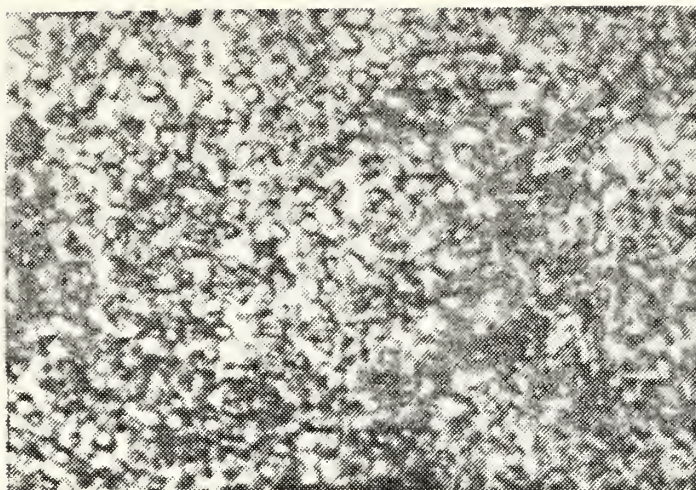
Rockwell C are theoretically possible (Ref. 14). However, high carbon steels are extremely brittle at room temperature, making machining and cold working extremely difficult. Additionally, these steels are very susceptible to cracking and distortion during heat treatment. To minimize these effects, the carbon steel is alloyed with elements which improve its toughness and hardenability without decreasing its wear resistance.

To produce AISI 52100 steel, a nominal one (0.98 - 1.10) weight percent carbon steel is alloyed with chromium (1.30 - 1.60%), manganese (0.25 - 0.45%) and silicon (0.15 - 0.30%) (Ref. 15). Chromium is a ferrite stabilizer which tends to raise the eutectoid (A_1) temperature and reduce the size of the austenite phase field in Figure 1 (Ref. 16). Also, chromium is a strong carbide former and grain refiner which tends to increase the hardenability of the steel especially when added in conjunction with small amounts of manganese, an austenite stabilizer, and silicon, another ferrite stabilizer (Ref. 17). Manganese is also a deoxidizing and desulfurizing agent and silicon is a deoxidizing agent, but the importance of these characteristics have been greatly minimized with the advent of melting techniques such as vacuum arc and electroslag remelting.

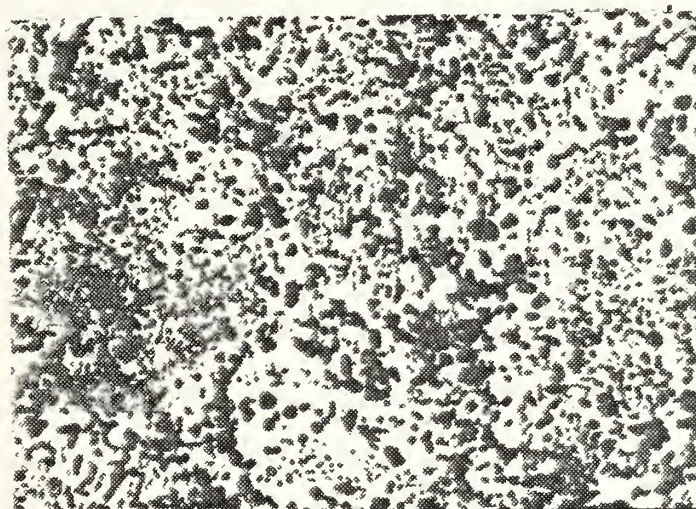
AISI 52100 steel is received from the steel mill in the form of hot rolled bars which have been given a spheroidizing anneal to produce microstructure consisting of spheroidal

carbides dispersed in a ferrite matrix (Fig. 4). This structure is preferred because it allows the material to be cut and machined with relative ease. Once worked to a rough shape, this structure is heat treated by austenitizing and subsequent quenching and tempering to obtain the desired levels of hardness and ductility.

Considerable research has been conducted to improve the mechanical properties of AISI 52100 steel, in particular the alloys resistance to fatigue failure. Much of this research has concentrated on improving heat treating techniques to obtain a microstructure consisting of fine martensite and an uniform dispersion of ultrafine (less than 1.0 microns) carbides. Grange [Ref. 18] proposed a technique for obtaining an ultrafine martensitic structure. This technique involved repeated cycles of rapid heating through the A_1 to just above the A_{cm} temperature, limiting the maximum temperature to that required for complete austenitization. This method of treatment refines the austenite grain size provided that the starting structure is a fine aggregate with only small carbides and no proeutectoid ferrite or cementite. Further grain refinement can be expected with each cycle until the instability of the ultrafine austenite prevents continued refinement and provided that the maximum temperature is reduced in each cycle. For alloy steels with greater than 0.9% carbon, complete austenitization is seldom possible, except by the use of very high austenitizing temperatures which result in excessive



(a)



(b)

Figure 4. Micrographs of as received AISI 52100 steel; (a) optical micrograph. Magnification 1000X. (b) TEM micrograph of carbon extraction replica. Magnification 1400X.

grain growth. Further, if the austenite has a carbon content greater than 0.8%, there will be some retained austenite in the hardened steel. The quantity of retained austenite will increase with increasing carbon content of the steel. However, if some degree of carbide dissolution is desired a carbide refining treatment must be performed prior to commencement of the cyclic rapid heat treatment. The resulting increase in the amount of retained austenite at the completion of the cyclic treatment then can be transformed by refrigeration and tempering prior to putting the piece into service.

The subject of carbide refinement has received increased attention since the advent of the high-speed gas turbine engine, in which the problem of rolling-contact fatigue has replaced wear as the life limiting factor of anti-friction bearing material. An examination of the effect of carbide size on the fatigue strength of AISI 52100 steel, tested on a rotating beam fatigue machine, was conducted by Monma et.al. [Ref. 19]. Their results indicated that a reduction of the mean carbide size from 1.4 microns to 0.56 microns increased the fatigue life by a factor of 2.5. In addition, their research revealed that up to 3 to 4 volume percent excess carbide actually improved the wear resistance of the bearing steel. This is similar to the work of Vincent et. al. [Ref. 20], who found that the presence of large oxide inclusions, from the melting stage, reduced rotating-beam fatigue life. Based on these results, Stickels [Ref. 21]

proposed a carbide-refining heat treatment which produced a microstructure consisting of 0.1 micron diameter carbides in a tempered martensite matrix. His treatment consisted of completely dissolving all carbides in the as received structure of AISI 52100 steel by high-temperature austenitization. The austenite was then isothermally transformed to produce a structure of bainite or pearlite, which was subsequently austenitized, quenched, and tempered in a conventional manner. The final result of this treatment is a uniform dispersion of ultrafine carbides. However, the as hardened structure tends to have greatly increased retained austenite. The transformation of this retained austenite to martensite by refrigeration, combined with the uniform dispersion of ultrafine carbides produces a harder structure, after hardening and tempering, than conventional heat treatment.

II. MATERIAL PROCESSING AND EXPERIMENTAL PROCEDURE

A. MATERIAL PROCESSING

The material used in the conduct of this research was aircraft quality, vacuum induction melt (VIM), consumable electrode vacuum arc remelt (VAR), AISI 52100 steel. It was obtained from two sources in the form of 8.9 cm (3.5 in.) diameter round bars which had been hot rolled to size and spheroidized annealed. The material designated 52100/0 was obtained from Vasco Pacific Steel and that designated 52100/2 from Carpenter Steel. Representative samples were sectioned from each as received bar for metallographic examination, hardness determination, and alloy chemistry determination. Material was also sectioned from material 52100/2 for later use in determination of standard properties and further heat treatment to provide a standard for comparison purposes. Specimens sectioned for the purpose of alloy chemistry determination were sent to Anamet Laboratories, Inc. of Berkeley, California, for chemical analysis. The results are presented in Table 1.

The material designated as 52100/0 was sectioned into lengths of 25.4 cm (10 in.) which were subsequently austenitized at 1000 degrees Celsius (1830 degrees F) for three hours then upset forged into blocks 7.6 cm (3.0 in.) by 5.1 cm (2.0 in.) by length. The blocks were allowed to air cool to less than 400 degrees Celsius (750 degrees F) and then were reheated to

650 degrees Celsius (1200 degrees F), held for two hours, and finally isothermally rolled to a true strain of approximately -2.3. This treatment schedule is shown schematically in Figure 5, with the time normalized to time per inch of specimen thickness. Henceforth, this treatment will be referred to as treatment B and specimens processed by this method will be designated specimen B, plus a numerical designation to signify the heat treatment.

Table 1. MATERIAL CHEMISTRY

<u>ALLOY ELEMENT</u>		<u>#52100/0</u>	<u>#52100/2</u>
Aluminum	(Al)	0.03%	0.03%
Carbon	(C)	1.00%	1.06%
Chromium	(Cr)	1.35%	1.37%
Columbium	(Cb)	0.005%	0.005%
Copper	(Cu)	0.11%	0.03%
Iron	(Fe)	Remainder	Remainder
Lead	(Pb)	0.005%	0.005%
Manganese	(Mn)	0.35%	0.36%
Molybdenum	(Mo)	0.06%	0.04%
Nickel	(Ni)	0.18%	0.07%
Phosphorus	(P)	0.007%	0.008%
Silicon	(Si)	0.27%	0.27%
Sulfur	(S)	0.007%	0.010%
Titanium	(Ti)	0.006%	0.006%
Tungsten	(W)	0.02%	0.17%
Vanadium	(V)	0.005%	0.02%

The material designated as 52100/2, with the exception of the material set aside for property determination and standard processing, was sectioned into lengths of 15.2 cm (6.0 in.) and heat treated in accordance with Figures 6 through 8 for treatments C through E respectively. The time scales for each of these treatment schedules is normalized to time per

TREATMENT B

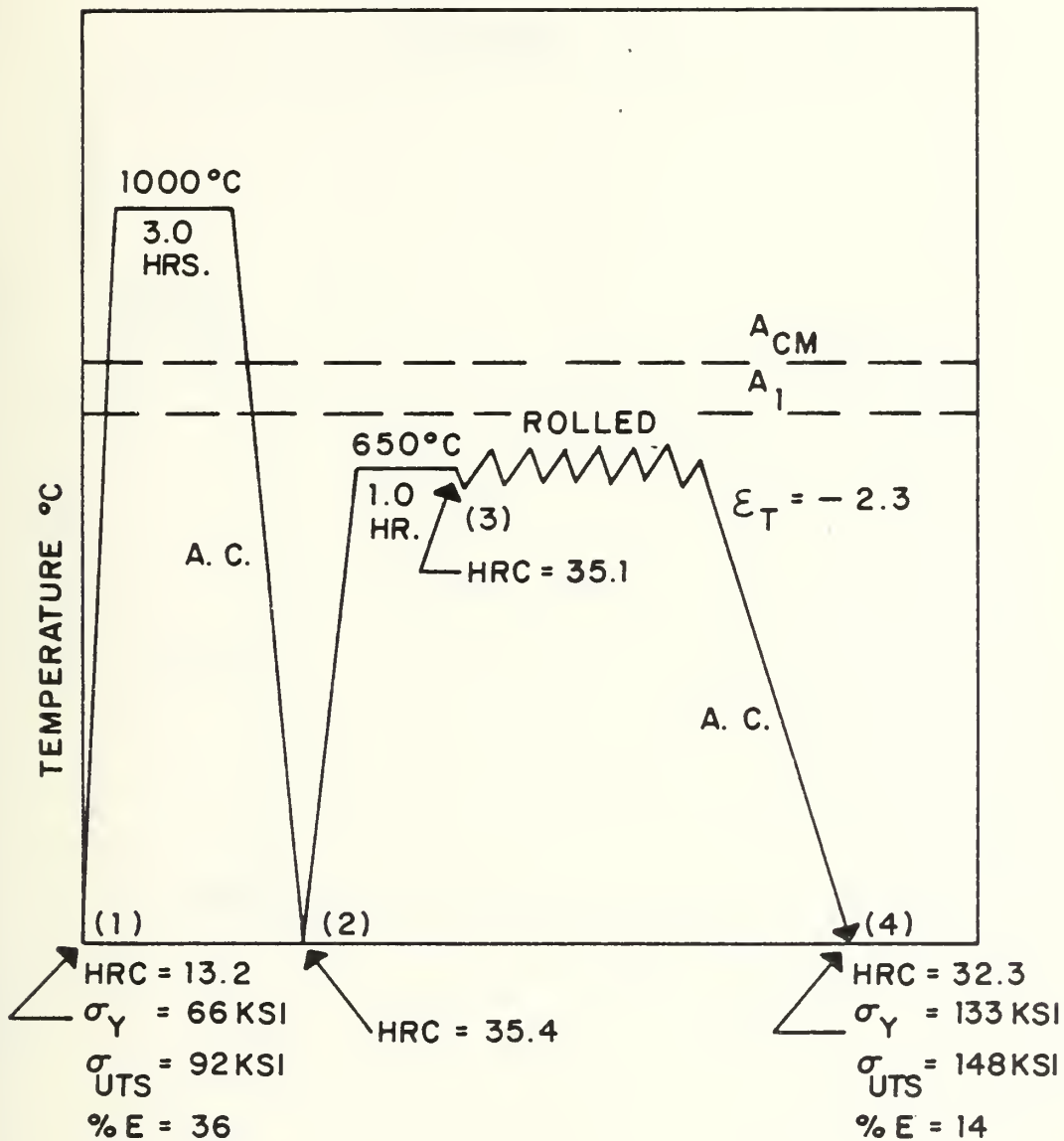


Figure 5. Schematic of Thermo-Mechanical Treatment-B.

TREATMENT C

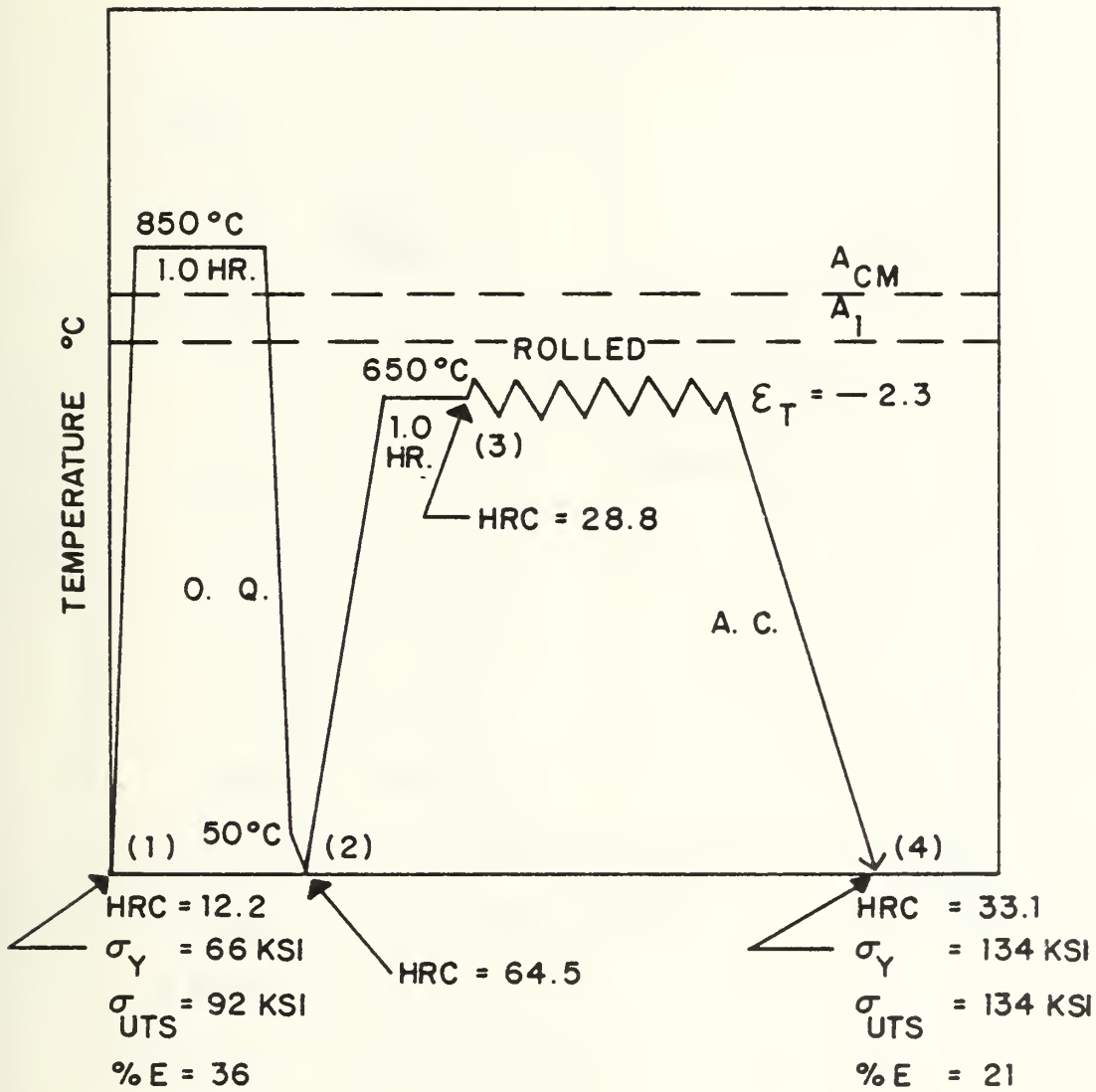


Figure 6. Schematic of Thermo-Mechanical Treatment-C.

TREATMENT D

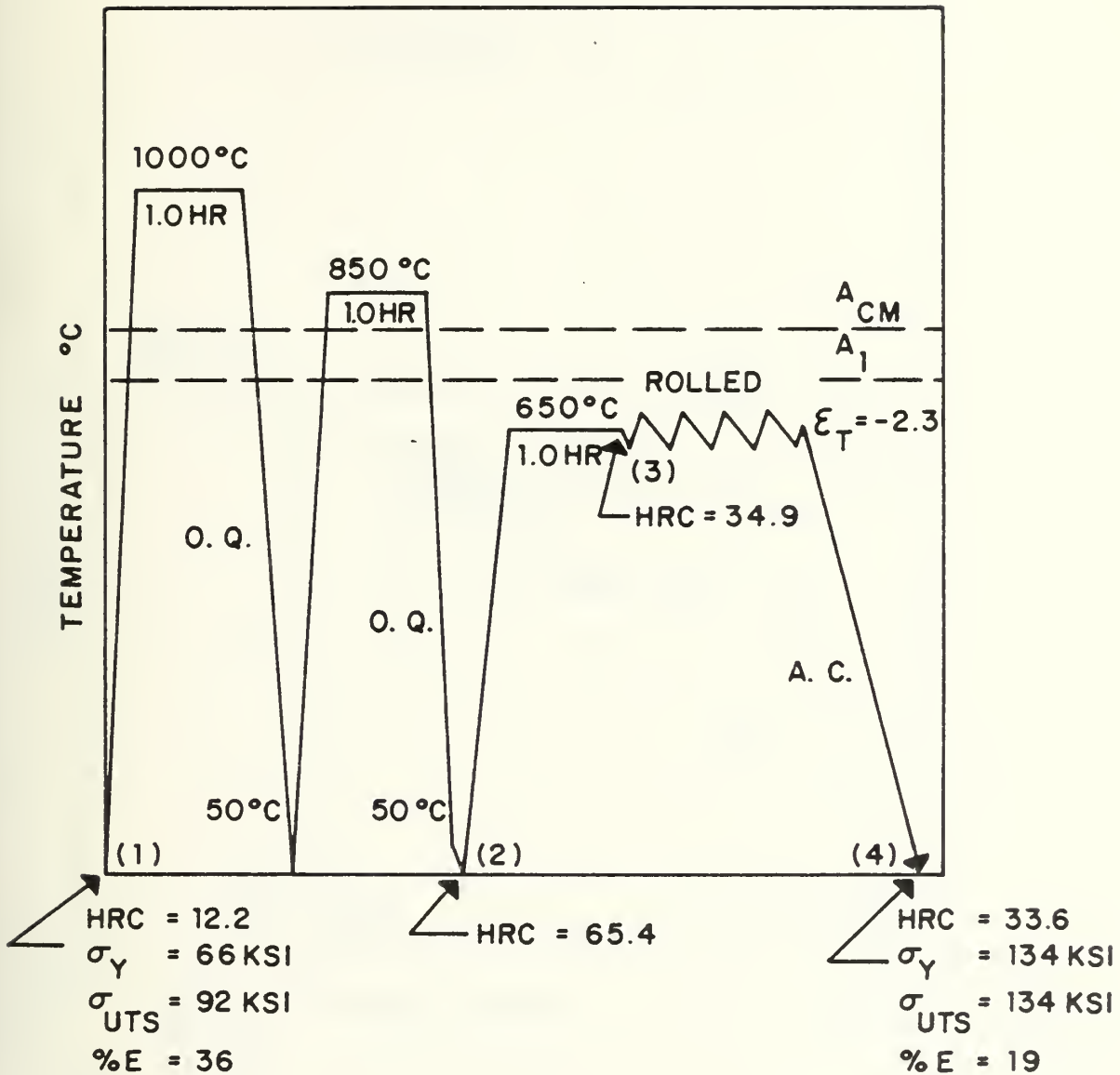


Figure 7. Schematic of Thermo-Mechanical Treatment-D.

TREATMENT E

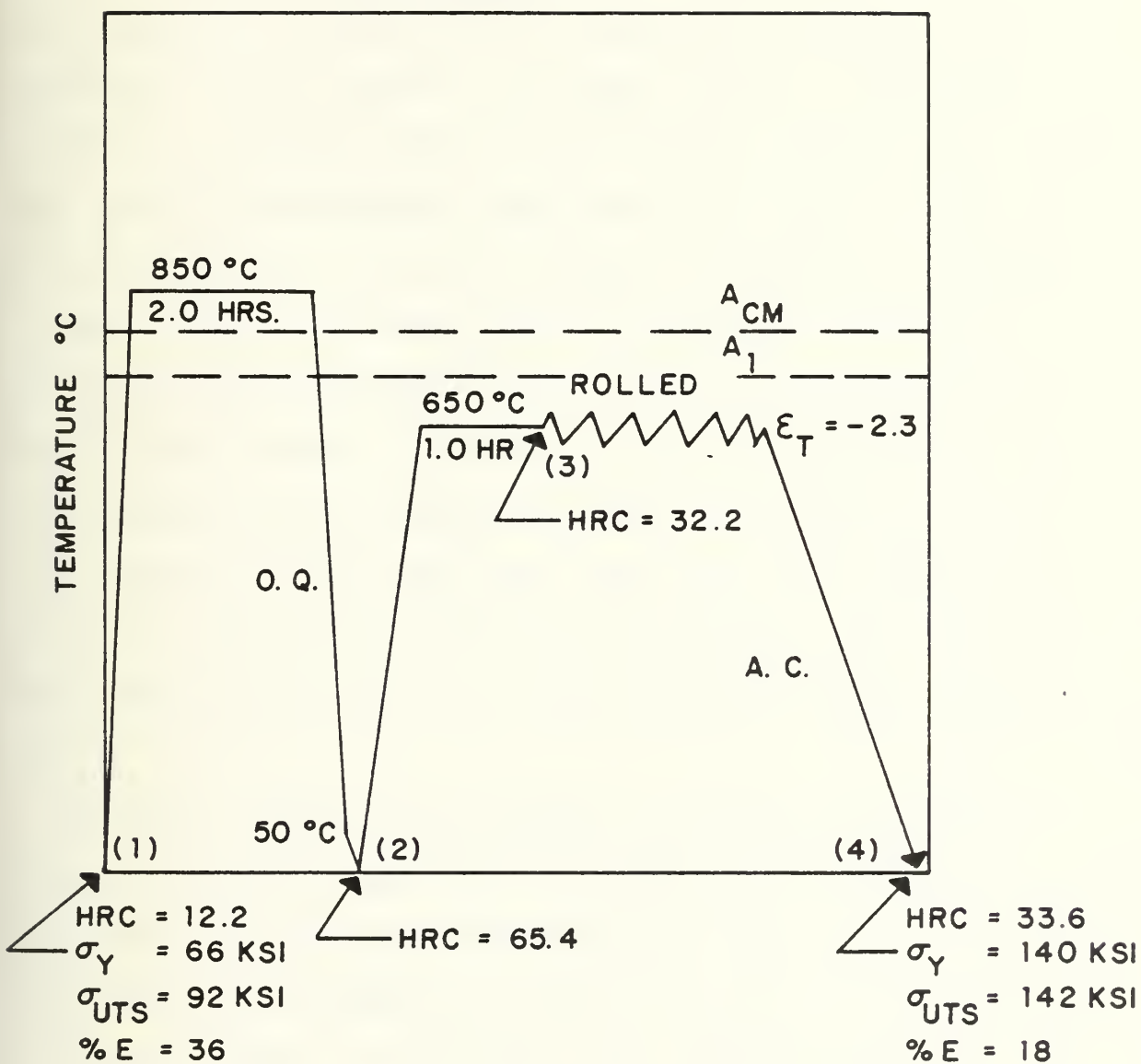


Figure 8. Schematic of Thermo-Mechanical Treatment-E.

inch of specimen thickness. These treatments were designed to provide various degrees of grain refinement and carbide dissolution. The prerolling austenitization was performed utilizing a Blue M box-type furnace with solid state proportioning controller, which maintained temperature to ± 5 degrees Celsius. The temperature was continuously monitored throughout the treatments using a Newport electronic digital thermometer utilizing a stainless steel sheath chromel-alumel thermocouple positioned at the specimen location on the hearth. Quenching was accomplished in warm oil located in containers adjacent to the furnace. As in the case of treatment B, the three additional heat treatments will henceforth be referred to by their letter and where necessary a number designation. The heat treated bars were then tempered at 650 degrees Celsius (1200 degrees F) for three hours and then upset forged into blocks 6.3 cm (2.5 in.) by 6.3 cm by length. The blocks were then isothermally rolled to a true strain of approximately -2.3.

The heat treatment of specimen B and the isothermal rolling of all specimens were performed at Viking Metals, Inc. of Richmond, California. The specimens were rolled in seventeen passes at a reduction of from 0.31 to 0.38 cm (0.12 to 0.15 in.) per pass. The pieces were reheated after each pass to 650 degrees Celsius. The reduction on the final pass was controlled to obtain the desired total true strain. The as rolled material was then allowed to air cool to room temperature.

The 52100/2 material to be used for property determination was normalized at 850 degrees Celsius (1560 degrees F) for seven hours which is the first step in the standard heat treatment recommended for AISI 52100 steel used in anti-friction bearings (Ref. 22). The specimens processed by this method are designated specimen A. The as treated material was sectioned longitudinally into flat plates approximately 0.76 cm (.30 in.) thick to facilitate further processing.

All specimens were then milled and/or surface ground to a thickness of 0.635 ± 0.005 cm (0.250 ± 0.002 in.), then cut into hardness coupons 3.8 cm by 1.0 cm by 0.635 cm (1.5 in. by 0.75 in. by 0.250 in.) and rectangular subsize tensile specimens according to ASTM specifications (Ref. 23).

B. EXPERIMENTAL PROCEDURE

1. Hardening Response

Hardness coupons from each of the five treatment groups were austenitized in a Lindberg Type CR-5 salt bath furnace, using neutral salt, for times ranging from 5 minutes to 1 hour at temperatures of 800 degrees Celsius (1470 degrees F), 825 degrees Celsius (1520 degrees F), and 850 degrees Celsius (1560 degrees F). Following austenitization, specimens were quenched in 50 degree Celsius (120 degrees F) oil then air cooled to room temperature. Each specimen was sectioned in half and one piece was set aside for hardness determination and microstructural (optical and TEM) examination. The other

half was refrigerated to -80 degrees Celsius (-112 degrees F) using ethanol in an FTS Multi-Cool, two stage refrigeration unit, to transform retained austenite present in the as quenched material. Twelve Rockwell-C hardness readings were taken on each specimen with a Wilson Rockwell Hardness Tester using a 150 kg load. The high and the low reading on each specimen were discarded and the statistical mean and standard deviation were calculated using an internal function of an HP41C calculator. The mean values were plotted as a function of austenitizing time at each temperature. Retained austenite measurements were made on specimens from groups A and B by McNelley et. al. at the Royal Military College of Science, Shrivenham, England using the spectrometer method discussed by Ogilvie [Ref. 24].

2. Tempering Response

Hardness coupons and tensile specimens were austenitized at 825 degrees Celsius in the same manner as described in the hardening response study and quenched in 50 degrees Celsius oil. The specimens were then tempered from 0.6 to 250 hours at temperatures of 175 degrees Celsius (345 degrees F), 350 degrees Celsius (660 degrees F), and 525 degrees Celsius (975 degrees F). The tempering was conducted in a Hoskins box type furnace with an Omega proportioning controller, which maintained temperature to ± 5 degrees Celsius. Specimens were air cooled from tempering temperatures prior to testing. Rockwell-C hardness readings were taken as previously described.

Tensile testing was conducted on specimens tempered at 350 and 525 degrees Celsius on a Materials Testing System Model 810 hydraulic test machine at the Materials and Molecular Research Division, Lawrence Berkeley Laboratory. The tensile specimens were loaded to failure using a ramp function at a strain rate of 8.3×10^{-4} sec. $^{-1}$. Tensile testing was not performed on specimens tempered at 175 degrees Celsius due to the nonavailability of grips capable of gripping material with hardnesses in excess of Rockwell-C 60. Hardness, elongation to failure, ultimate tensile and yield strength were recorded and plotted as a function of time for each tempering condition. The data was normalized using a least square method contained in the curve fitting routine contained in the standard applications module for the PH41C calculator.

3. Optical Microscopy

Specimens were sectioned at various points throughout the processing and hardening studies for metallographic examination. They were mounted and ground through 600 grit using a Buehler Automet grinding and polishing unit and metallographically prepared with 1 micron diamond paste. After polishing, the specimens were ultrasonically cleaned in an ethanol bath and the polished surface etched in a 1% Nital solution. Etching times varied from 5 seconds to one minute. Optical photomicroscopy was then conducted on a Zeiss Universal photomicroscope.

4. Transmission Electron Microscopy

Transmission electron microscopy was conducted on both carbon extraction replicas and thin metal foils using a Philips EM201 transmission electron microscope at Stanford University's Hopkin Marine Station. Specimens for the carbon extraction replication were mounted and metallographically prepared through 1 micron diamond paste. The polished surface was lightly etched in a 1% Nital solution. Carbon was evaporated onto the surface under a vacuum of approximately 6×10^{-5} torr. in a Fullam Model 1250 EFFA Evaporator. A current of 50 amps and a burn time of three seconds was used. The surface of the specimen was then sectioned into squares, 3 mm on a side, and the specimen was immersed in a solution of 10% Nital to loosen the replica. The replica was then floated off the surface in an aqueous solution containing 3% ethanol and retrieved on a 3 mm diameter grid and allowed to dry prior to microscopic examination. This method of replication of high carbon steel was suggested by A. Doig at the Royal Military College of Science (Ref. 25).

Specimens for thin foils were sectioned in wafers 0.38 - 0.51 mm (0.015 - .020 in.) thick using a Buehler Isomet low speed saw equipped with a low-concentration diamond blade. Utilizing a wet belt sander and wet static papers (240 - 600 grit), the wafers were further ground to a thickness of 0.13 - 0.18 mm (0.005 - 0.007 in.) from which 3 mm disks were obtained. The disks were then thinned to penetration using a 5% perchloric-acetic acid electrolyte in a modified Buehler Electromet

jet thinner. A jet speed setting of 3 to 5 was used with a 70 volt DC potential giving a thinning current from 15 to 30 mA. The penetrated foils were then cleaned in ethanol and dried prior to microscopic examination. Thinning times ranged from seven to twelve minutes depending on the initial thickness of the disk.

III. RESULTS AND DISCUSSION

A. EFFECT OF PRE-ROLLING TREATMENT AND ROLLING

1. Mechanical Test Results

Mechanical testing was performed at each step of the thermo-mechanical treatments shown previously in Figures 5 through 8. Tensile testing and hardness determination were conducted on the as-received and as-treated condition of each of the thermo-mechanical treatments. Additionally, the hardness was determined at the two intermediate conditions. These results are tabulated in Table 2 and indicated in Figures 5 through 8, for each step of the various thermo-mechanical treatments. The as-rolled hardness of the treated material ranged from 32.3 to 33.6 Rockwell-C, compared to a hardness of 23.4 Rockwell-C for the unrolled treatment-A (normalized from 850 degrees Celsius). The treated materials also exhibited significantly higher yield strengths in comparison to treatment-A. Additionally, during tensile testing it was observed that once yielding occurred treatments C, D, and E did not exhibit a typical response to continued loading. The load versus elongation curves for these treatments did exhibit the typical upper and lower yield points common to most body centered cubic materials, but showed no significant work-hardening after yielding. The Luder bands, once formed, appeared to pass through the gauge length in a series of distinct wave

fronts until failure occurred. This response was not observed in the treatments A and B, which exhibited the normal elastic-heterogeneous plastic-homogeneous plastic response common to most body-centered cubic ferrous materials. These results are compared and summarized in Figure 9.

Table 2. THERMO-MECHANICAL TREATMENT-MECHANICAL TEST DATA

TREATMENT	STEP	HARDNESS (Rockwell-C)	YIELD (MPa/Ksi)	TENSILE (MPa/Ksi)	PERCENT ELONGATION
B	1	13.2	455 / 66	634 / 92	36
B	2	35.4	-----	-----	--
B	3	35.1	-----	-----	--
B	4	32.3	917 / 133	1020 / 148	14
C	1	12.2	455 / 66	634 / 92	36
C	2	64.5	-----	-----	--
C	3	28.8	-----	-----	--
C	4	33.1	924 / 134	924 / 134	21
D	1	12.2	455 / 66	634 / 92	36
D	2	65.4	-----	-----	--
D	3	34.9	-----	-----	--
D	4	33.6	924 / 134	924 / 134	19
E	1	12.2	455 / 66	634 / 92	36
E	2	65.4	-----	-----	--
E	3	32.2	-----	-----	--
E	4	33.6	965 / 140	979 / 142	18

2. Optical Microscopy Results

Optical microscopy was performed at each step of the thermo-mechanical treatments. The fineness of the as-rolled structures prevents detailed examination of these structures. However, the general structural response of the material to

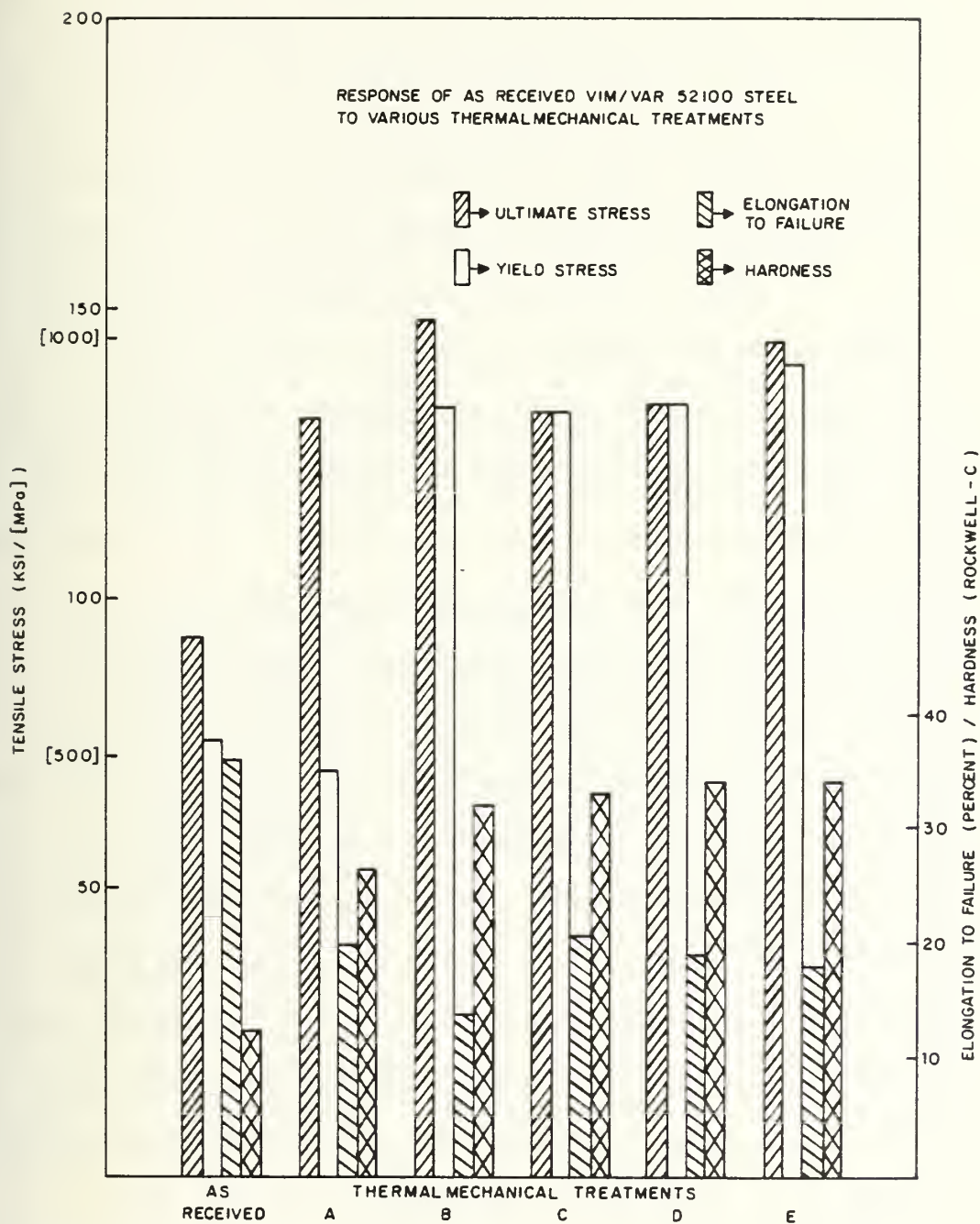
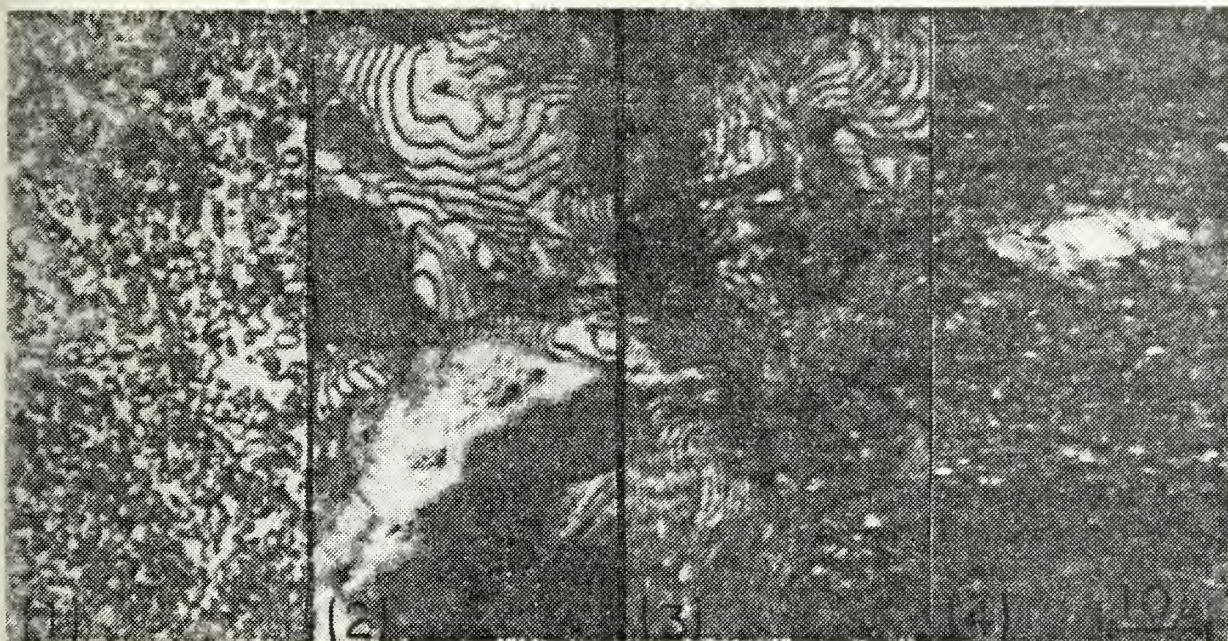


Figure 9. Comparison of Thermo-Mechanical Treatments.

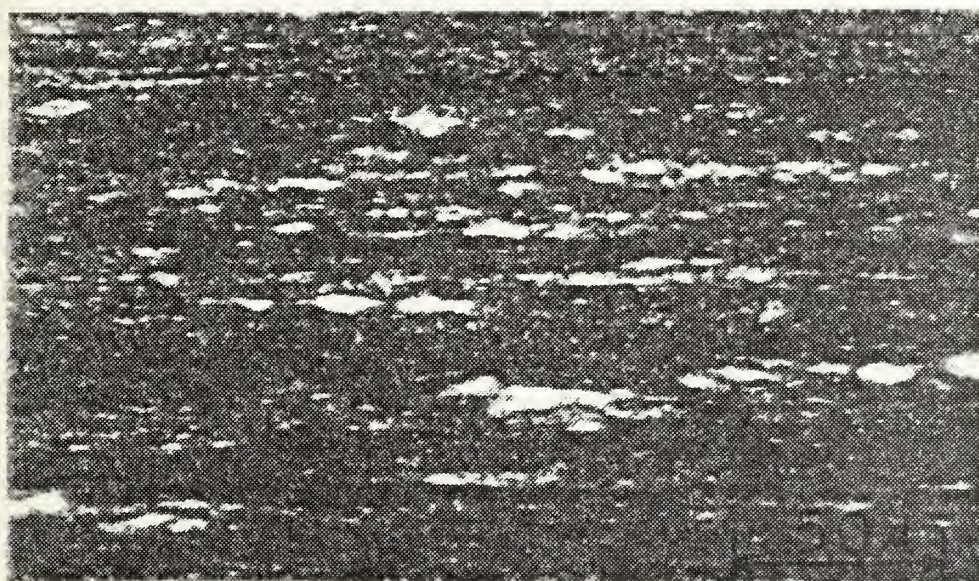
the various treatments is observable, in particular the distribution of the optically resolvable carbides. These carbides will be subsequently referred to as residual carbides, since they remained undissolved after initial heat treatment. The presence of carbides smaller than approximately 0.5 microns and the exact diameter of such carbides could not be determined due to the depth of field and resolving capabilities of the optical microscope.

The general structural response of AISI 52100 to thermo-mechanical treatment-B is shown in Figure 10a (numbers in the lower left corner of each section of the micrograph indicates the step number of the treatment). It is evident from this series that the structure is greatly refined by the rolling process. However, the presence of relatively large pearlitic regions and the microstructural banding resulting from the break up and refinement of the proeutectoid grain boundary carbides indicate that the deformation was insufficient to totally refine the as treated starting structure (step 2). This is evident in Figure 10b. The relatively large, irregular white regions are pearlitic regions unresolvable at this magnification and the smaller somewhat more regular shaped particles are residual carbides.

The general structural response of the material to treatment-C is shown in Figure 11. The microstructure (Fig. 11a) consists predominately of fine-grained martensite and had a hardness of 64.5 Rockwell-C. Since the hardness

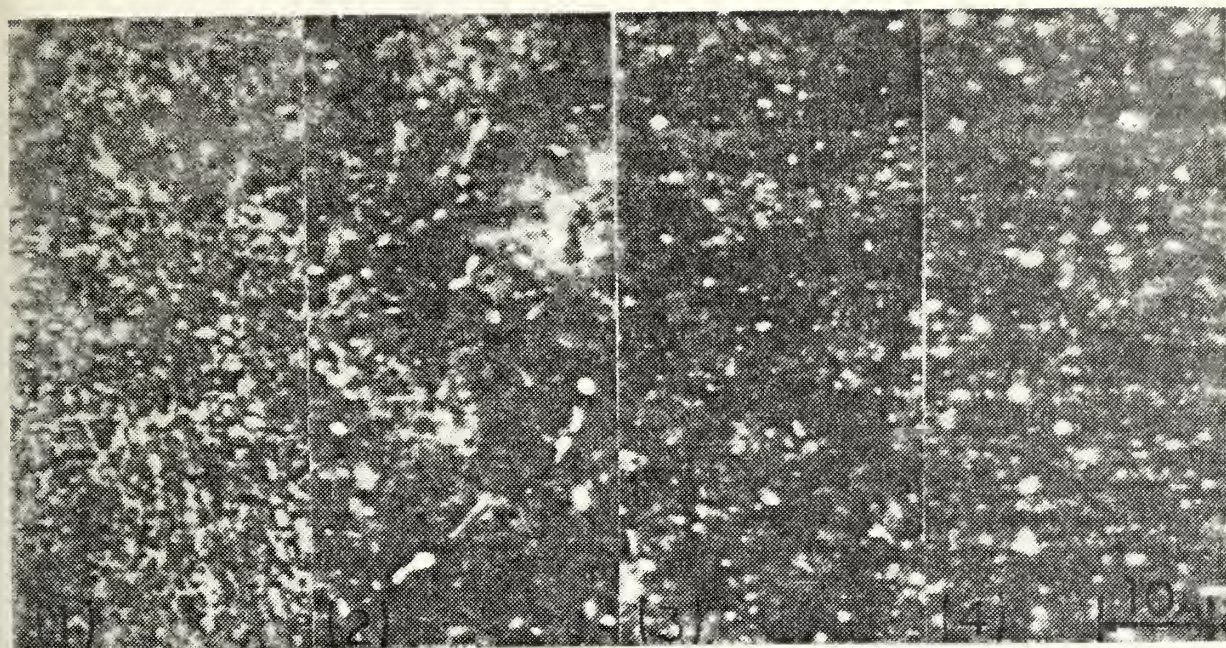


(a)

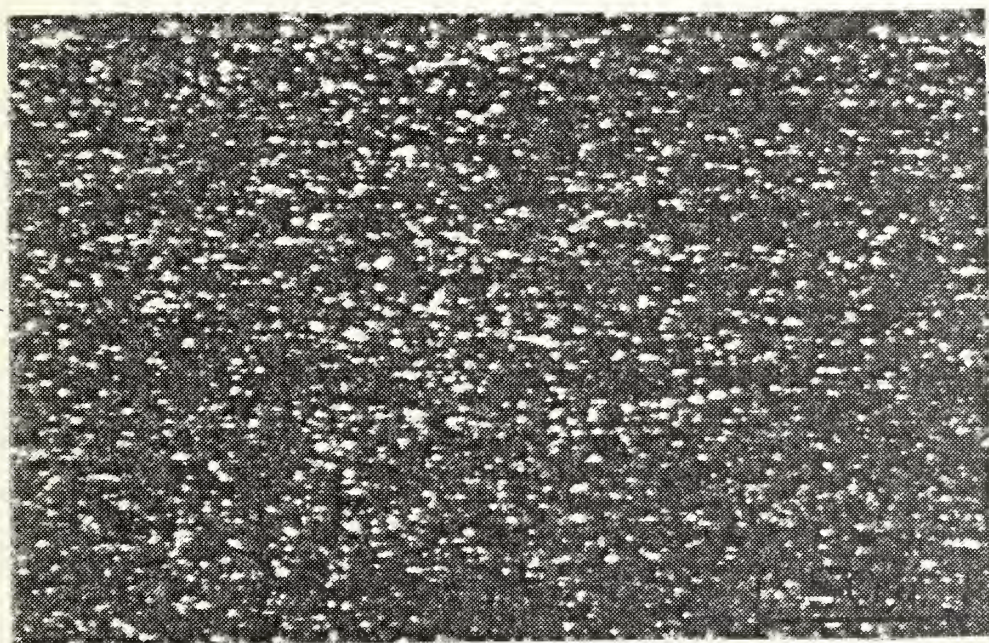


(b)

Figure 10. Microstructural Effect of Treatment B: (a) Magnification 1000X; (b) Magnification 250X.



(a)

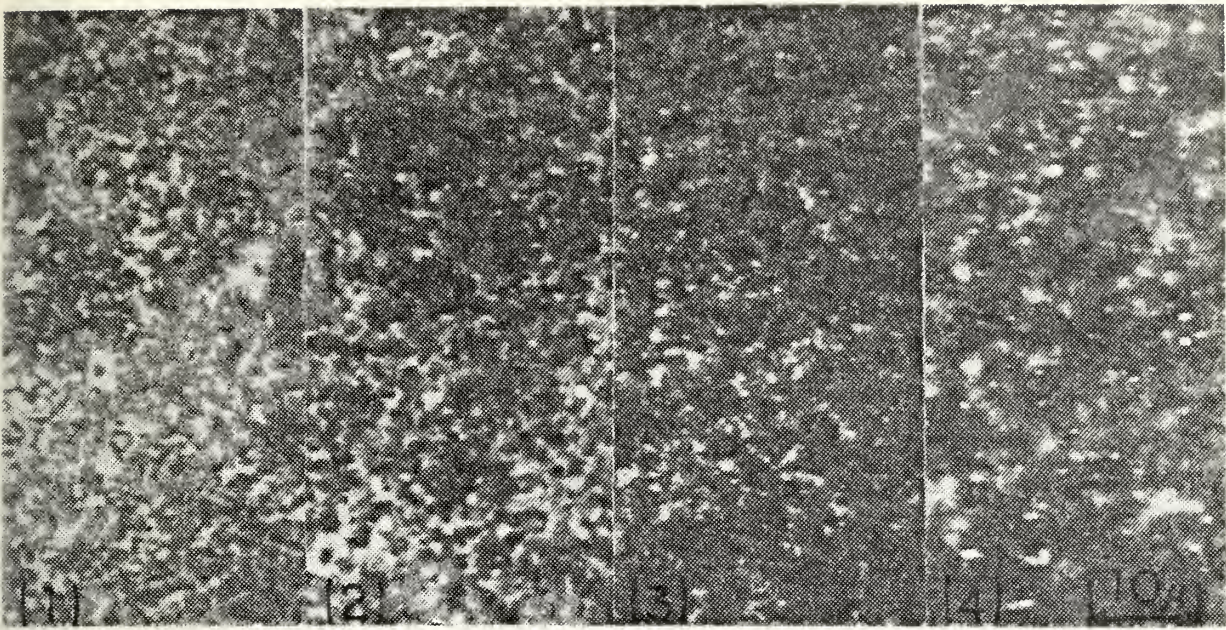


(b)

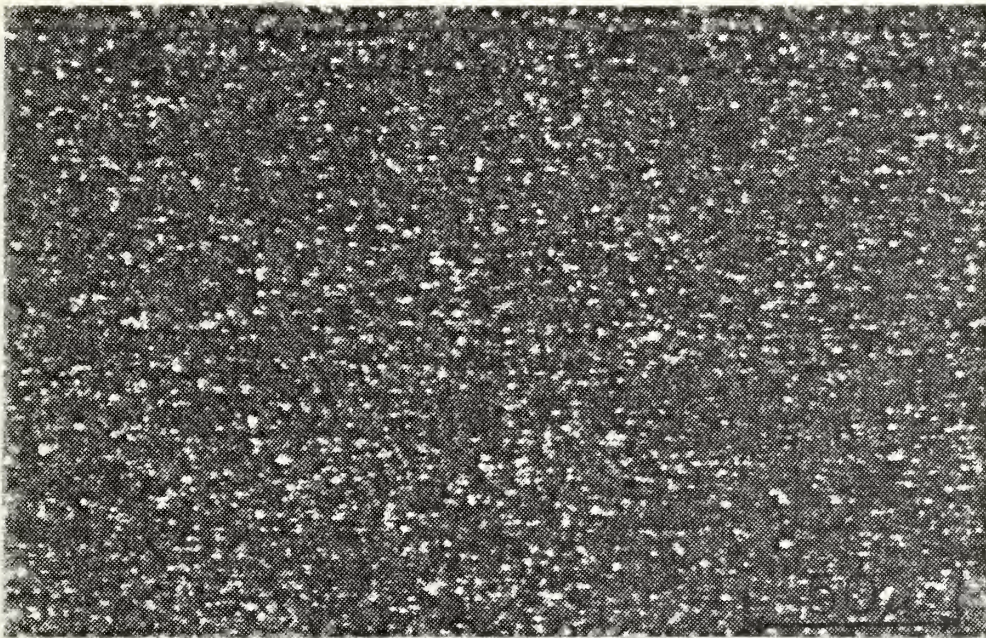
Figure 11. Microstructural Effect of Treatment C: (a) Magnification 1000X; (b) Magnification 250X.

increased after refrigeration, there is also some retained austenite. Because the quench into warm oil is not as severe as a normal oil quench, some of the austenite may have transformed to lower bainite. The size of the residual carbides at this step are somewhat larger than those in treatment-B. This is a result of the lower austenitization temperature and shorter time at temperature utilized in treatment-C. Also evident in this figure are the prior austenite grain boundaries (step 3), which are characterized by the darker regions in the structure (Ref. 26). The overall refinement obtained through treatment-C appears to be similar to that of treatment-B with the exception that the banding observed in B is not evident in C (Fig. 11b). Banding of proeutectoid cementite has been regarded as detrimental to rolling contact fatigue (Ref. 27). Its absence in steels processed as treatment-C would be beneficial.

In an effort further to refine the microstructure of the material prior to isothermal rolling, treatments utilizing multiple austenitizing cycles (treatment-D) and extended time at temperature (treatment-E) were studied. The as-treated hardness of both treatments was measured to be 65.4 Rockwell-C. The microstructural effect resulting from treatment-D and E is shown in Figures 12a and 13a respectively. The solutioning of the carbides appears to be more complete in these treatments, with treatment-D being slightly more effective than E.

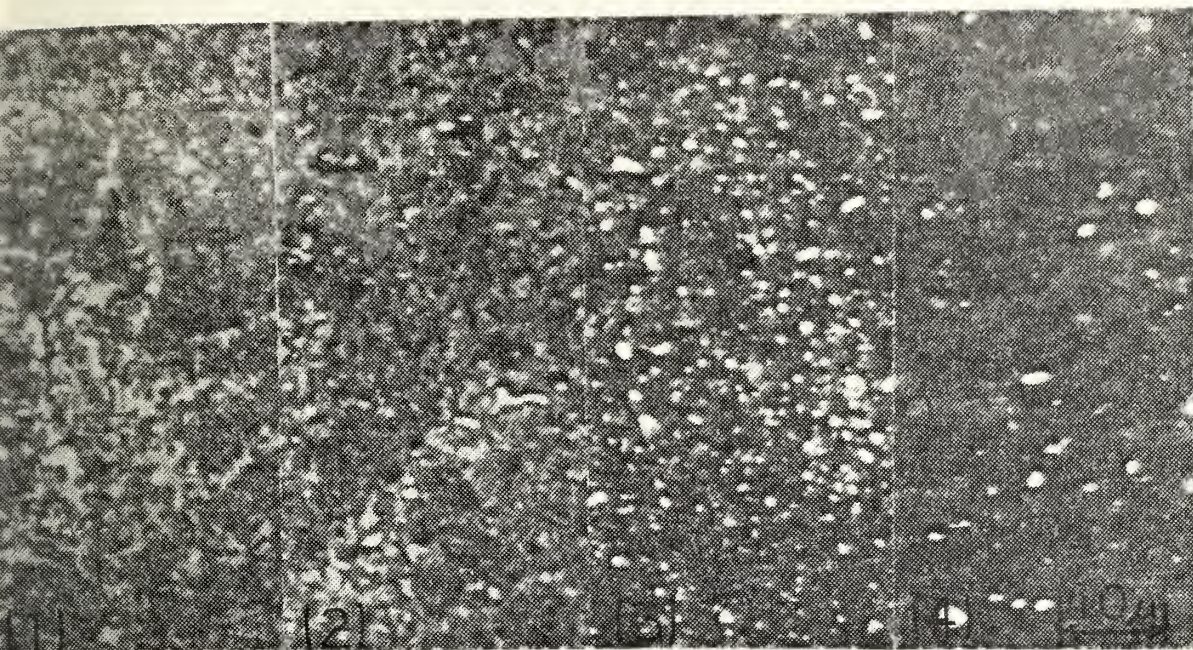


(a)

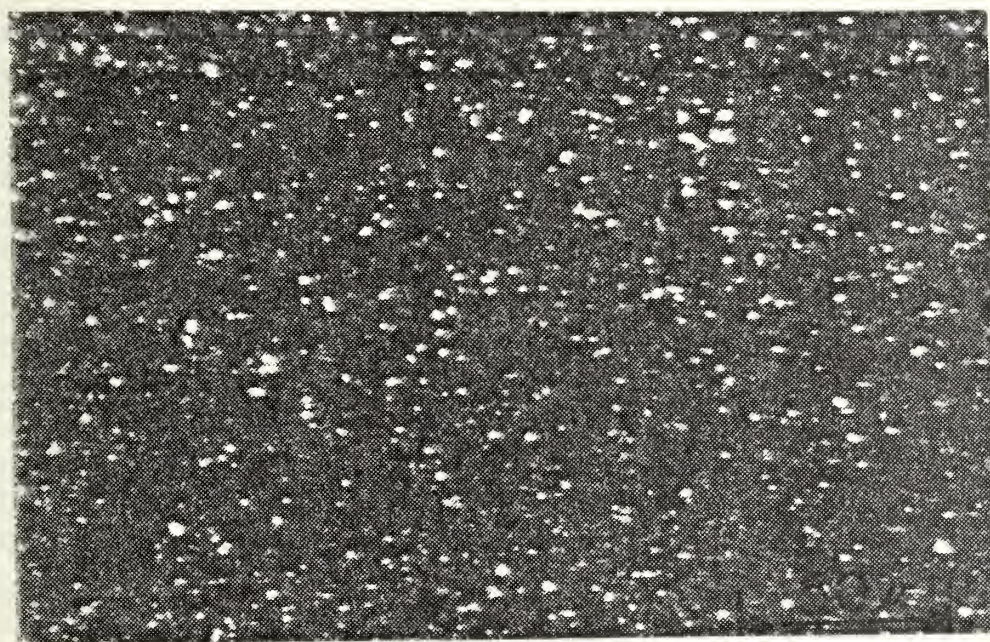


(b)

Figure 12. Microstructural Effect of Treatment D: (a) Magnification 1000X; (b) Magnification 250X.



(a)



(b)

Figure 13. Microstructural Effect of Treatment E: (a) Magnification 1000X; (b) Magnification 250X.

This is thought to be a result of the higher initial austenitizing temperature utilized in treatment-D. However, the resulting slightly higher carbon content of the as rolled matrix was not sufficient to increase the measured hardness because this effect is masked by the increased retained austenite content observed in finer as-quenched microstructure (Ref. 21). The distribution of the residual carbides resulting from these treatments appears to be somewhat similar with the exception that treatment-E exhibits a slightly coarser and more sparse distribution. The coarsening observed in treatment-E possibly results from the extended time at austenitizing temperature as reported by Stickels (Ref. 21). The structures obtained from treatments D and E appear to be more refined and uniform, as shown in Figures 12b and 13b, than that obtained from treatment-C. Any improvement in the fatigue or fracture toughness properties of these treatments when compared to treatment-C are expected to be slight because of the relatively small difference in the size of the residual carbides is small (Ref. 19). In addition, the higher carbon content of the austenite and the likelihood of increased volume percent retained austenite increase the probability of quench cracking.

3. Transmission Electron Microscopy Results

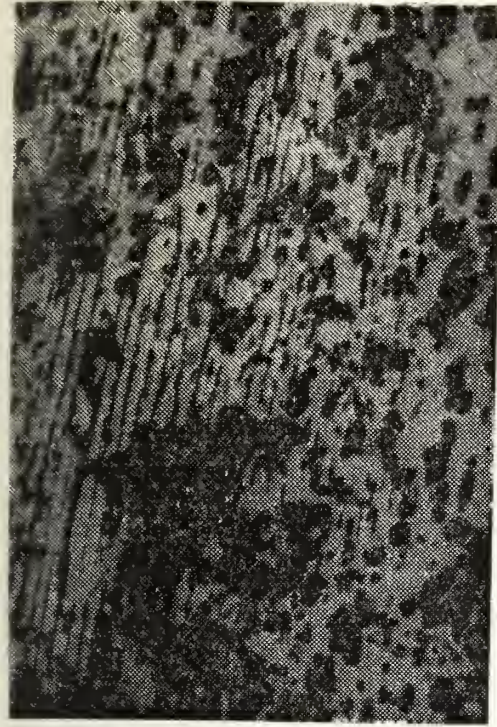
Transmission electron microscopy was utilized to further examine the pre-rolling (step 3) and the post-rolling (step 4) structures. The carbon extraction replica method

was used on treatments B through E. Due to the coarseness of the pre-rolled structure of treatment-B, replicas could not be obtained from this step. In addition to the carbon extraction replicas, thin foil specimens were obtained of the pre-rolling condition of treatment-C and the post-rolling condition of treatments B and C.

The carbon extraction replicas of treatment-B confirm the fine carbide distribution and the coarse banded structure observed optically. Additionally these high magnification micrographs revealed the presence of extremely fine pearlite and the breakup of the pearlite to form equally fine spheroidal carbides. This effect is shown in Figure 14, which shows this post-rolling structure from 5,000 to 15,000X magnification. The micrographs taken of the thin foil specimens are shown in Figure 15a and b at magnifications of 20,000 and 45,000X respectively. The size of the carbides revealed by these micrographs ranges from less than 0.1 to approximately 0.3 microns with an average grain size of 0.3 to 0.5 microns. The remnants of the proeutectoid cementite do not appear in these micrographs. However, the pearlite structures present in Figure 15 a, when compared to that shown in Figures 10a(4) and 14, show the presence of pearlite colony sizes ranging from 10 microns down to less than 1.0 microns with a lamellar spacing as small as 0.05 microns. The ultrafine equiaxed grains present in these micrographs appear to have varying



(a)



(b)



(c)

Figure 14. Carbon Extraction Micrograph of Treatment-B (as rolled): (a) Magnification 5,000X; (b) Magnification 10,000X; (c) Magnification 15,000X. Structure shows distribution of carbides.

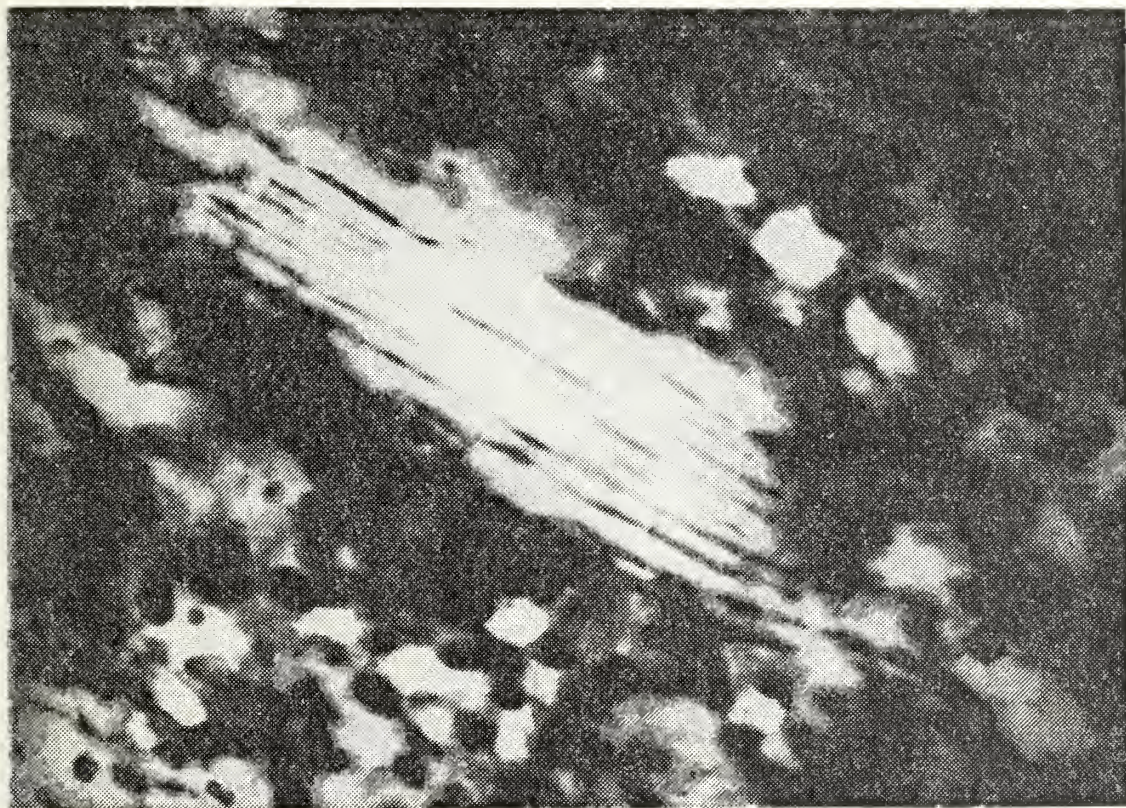


Figure 15a. Transmission Electron Microscope Thin Foil Micrograph of As-Rolled Treatment B. Micrograph shows ultrafine pearlite and ultrafine carbides dispersed in equiaxed matrix. Magnification 20,000X.

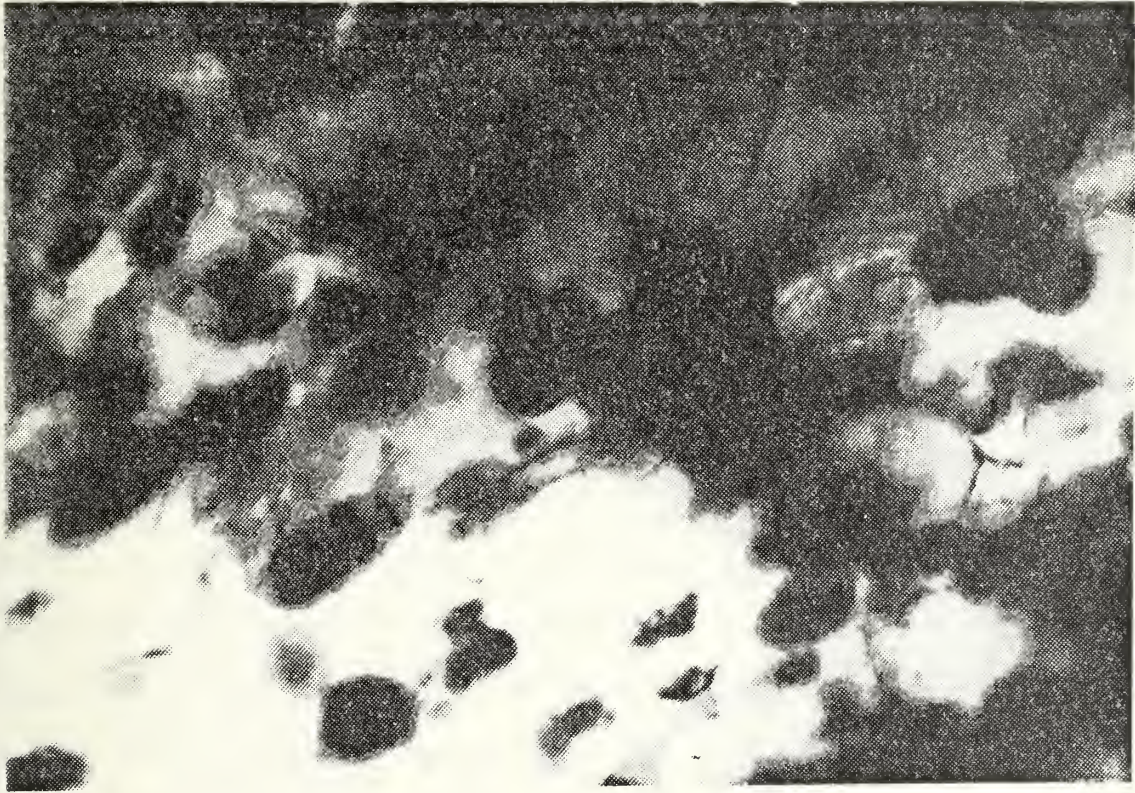


Figure 15b. T.E.M. Thin Foil Micrograph of As-Rolled Treatment-B. Micrograph shows carbide distribution and dislocation density in equiaxed grain structure. Magnification 45,000X.

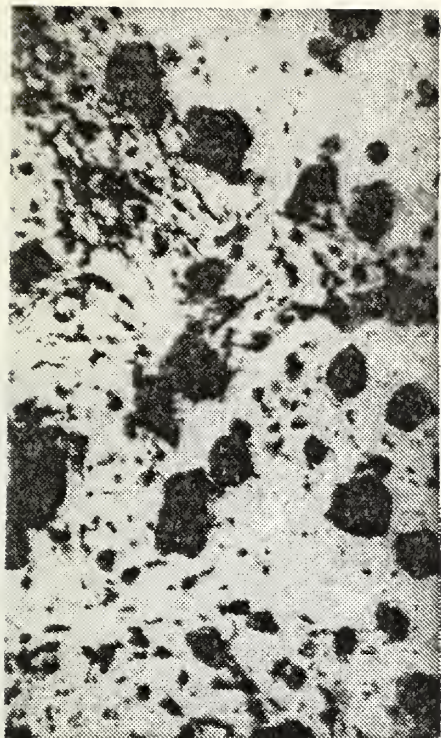
dislocation densities. Some grains are relatively strain-free, while other have higher densities, more characteristic of cold-worked material.

Carbon extraction replicas were taken from both the pre-rolling and post-rolling conditions of treatment-C, and subsequent treatments. The pre-rolling micrographs of treatment-C are shown in Figure 16. Two distinct carbide sizes are present. The larger carbides, on the order of 1.0 micron in size, are the result of incomplete dissolution during austenitization (residual carbides), while the small carbides appear to be the result of the 650 degree Celsius temper conducted prior to the rolling process (steps 2 to 3). The presence of these smaller carbides is confirmed and their approximate size can be determined from the then foil micrographs, Figure 17. These ultrafine carbides appear predominately along visible grain and subgrain boundaries, and range in size from less than 0.03 microns to slightly larger than 0.1 microns. The structure visible in Figure 17b appears to have a relatively low dislocation density and dislocations as located primarily in the regions surrounding the grain boundary carbides. Grain size ranges from 0.4 to 0.8 microns.

Carbon extraction replica micrographs of treatment-C in the as rolled condition are shown in Figure 18. These micrographs clearly indicate the presence of two distinct sizes of carbide particles, with the larger particles being



(a)



(b)



(c)

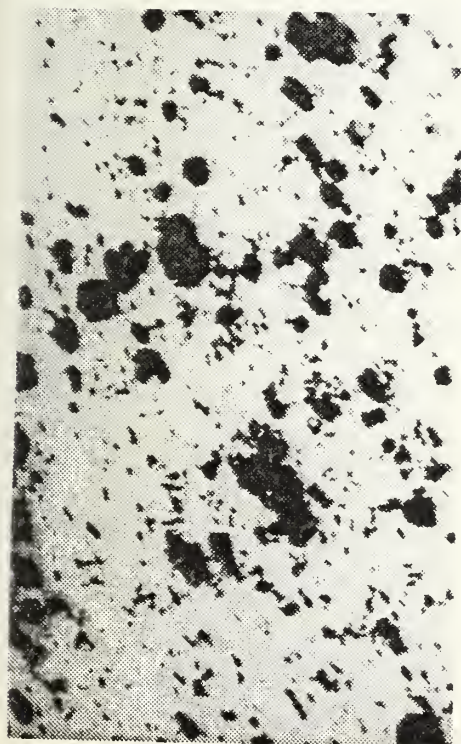
Figure 16. Carbon Extraction Micrograph of Treatment -C (prior to rolling): (a) Magnification 5,000X; (b) Magnification 10,000X; (c) Magnification 15,000X. Structure shows distribution of carbides.



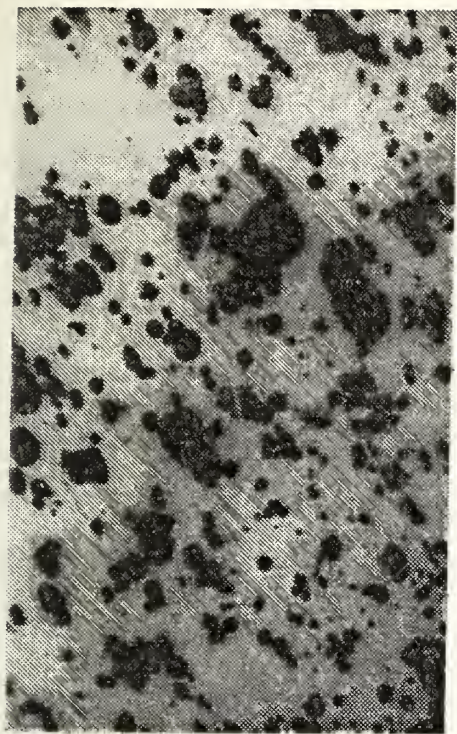
Figure 17a. Transmission Electron Microscope Thin Foil Micrograph of Treatment-C Prior to Rolling. Micrograph shows two distinct size carbide particles dispersed in matrix. Magnification 20,000X.



Figure 17b. T.E.M. Thin Foil Micrograph of Treatment-C Prior to Rolling. Micrograph shows carbide distribution and dislocation pile ups in region of grain boundary carbide. Magnification 45,000X.



(a)



(b)



(c)

Figure 18. Carbon Extraction Micrograph of Treatment-C (as rolled): (a) Magnification 5,000X; (b) Magnification 10,000X; (c) Magnification 15,000X. Structure shows distribution of carbides.

slightly smaller than the residual carbides present in the pre-rolling condition. This indicates only a slight reduction in residual carbide size as a result of the rolling process. The smaller carbides present in the pre-rolled structure appear to have coarsened slightly and become more uniform in size and distribution in the as-rolled structure. This indicates that the tempering conducted prior to rolling was incomplete in that the carbon content of the martensite had not reached equilibrium. The fact that these particles are approaching a uniform size suggests that during rolling the tempering process is continuing towards equilibrium. The thin foil micrographs of this structure are shown in Figure 19a. Examination of these microstructures confirms the coarsening of these ultrafine carbides and clearly shows the role of these carbides in inhibiting growth of the ultrafine grains produced by the thermo-mechanical treatment. The as-rolled grain size, as shown in Figure 19b, is about 0.2 to 0.3 microns with an average ultrafine carbide size of between 0.05 to 0.1 microns. Also, the dislocation density of the as-rolled grains suggest that recrystallization is occurring during the rolling process. This is indicated by the presence of heavily dislocated grains adjacent to relatively strain-free grains. The grain size after thermo-mechanical treatment is extremely fine, and suggests that there was very little grain growth after recrystallization, due to the presence of the ultrafine carbides at the grain boundaries.

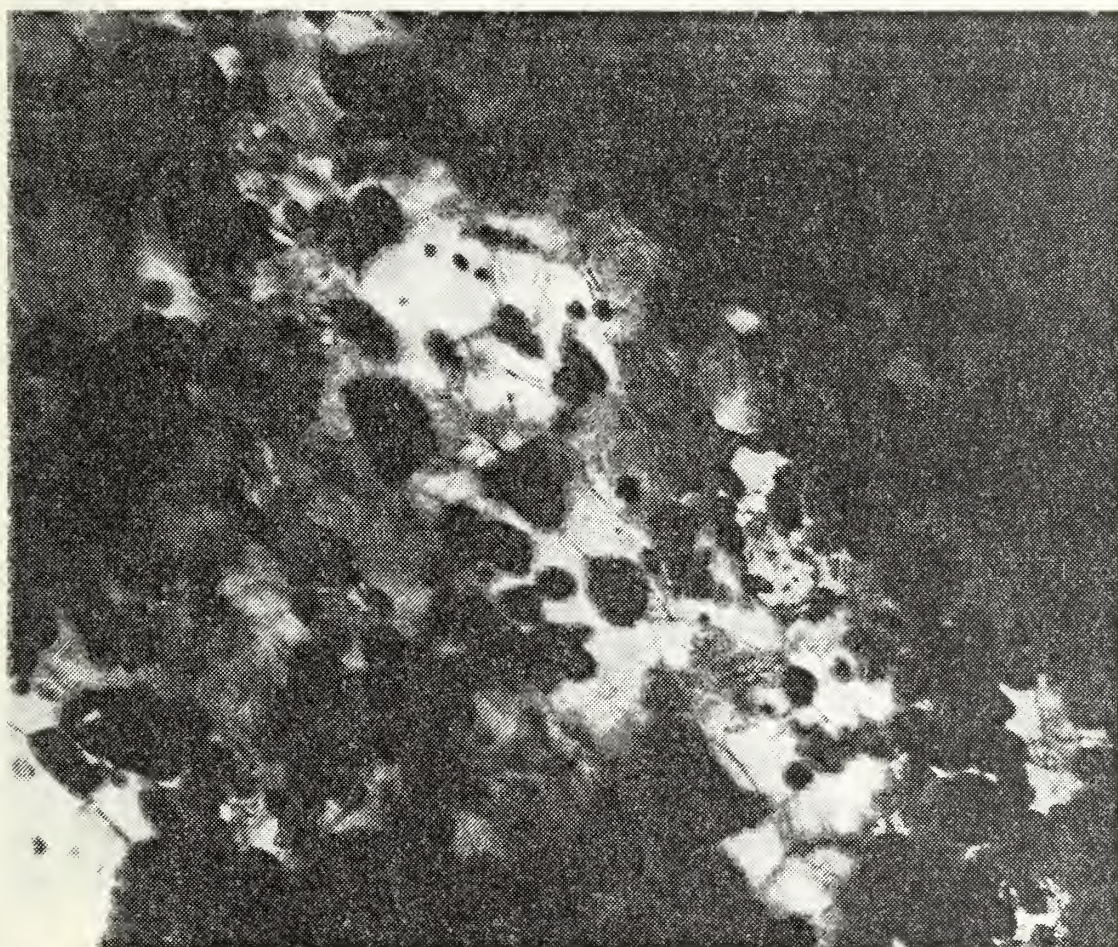


Figure 19a.

Transmission Electron Microscope Thin Foil Micrograph of As-Rolled Treatment-C. Micrograph shows refined grain structure and carbide distribution as a result of isothermal rolling. Note the two distinct carbide sizes. Magnification 20,000X.

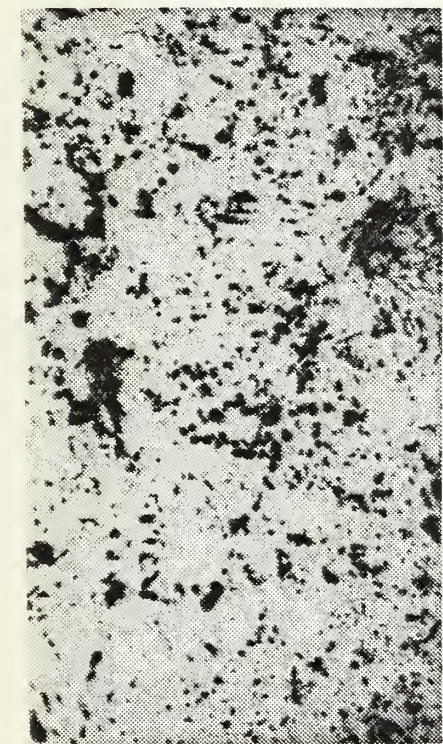


Figure 19b. T.E.M. Thin Foil Micrograph of As-Rolled Treatment-C. Micrograph shows grain size and dislocation density. Note location of small carbides in grain boundaries and that some grains appear to be relatively strain free while others are heavily dislocated. Magnification 45,000X.

Carbon extraction replicas were also produced and examined from the pre-rolling and post-rolling conditions of treatments D and E. These micrographs are shown in Figures 20 through 23 respectively. These structures correspond well with the optical micrographs shown in Figures 12 and 13 respectively. However, the higher magnification and different specimen preparation techniques used allow for examination of the optically unresolvable carbides. The presence of the two distinct size carbide particles and the coarsening of the residual carbides with increased time at austenitizing temperature as reported by Stickels Ref. [21] is clearly evident. The nucleation and growth of the smaller carbides that result from the tempering of the previously martensitic structure is also very evident, especially when comparing the structures in Figures 22 and 23.

4. Summary of Effects

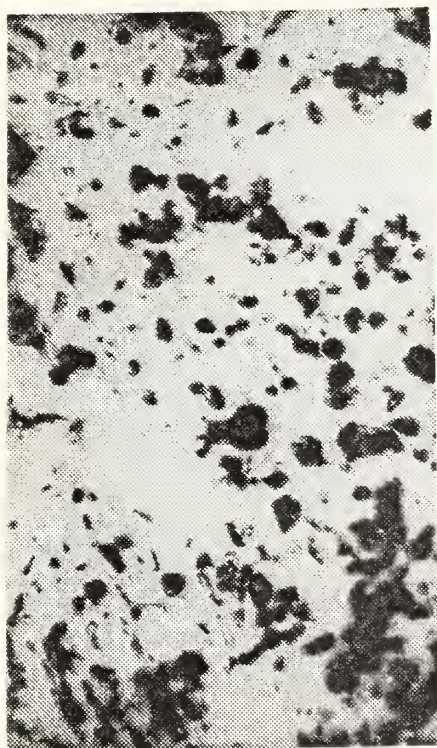
Thermo-mechanical treatment to this stage of processing produces an ultrafine grain structure with a dispersion of ultrafine carbides and somewhat large residual carbides interspersed throughout, provided that the starting structure is martensitic or a combination of martensite and bainite. Significant microstructural refinement is obtained from normalized structures consisting of coarse pearlite and proeutectoid grain boundary cementite. However, the thermo-mechanical processing does not completely break up and refine these structures and, combined with the incomplete solutioning



(a)

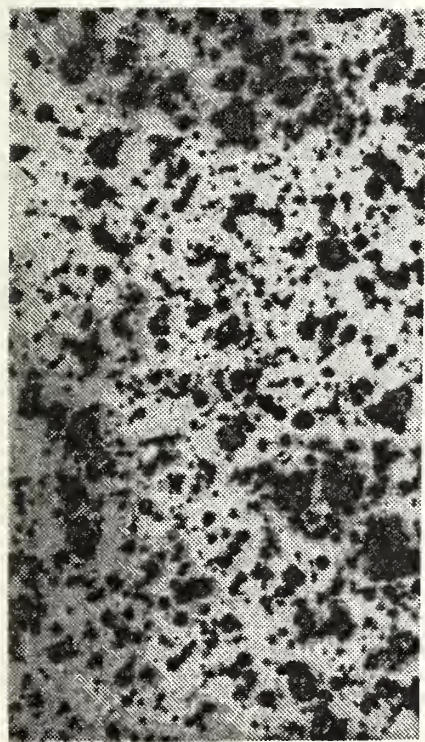


(b)

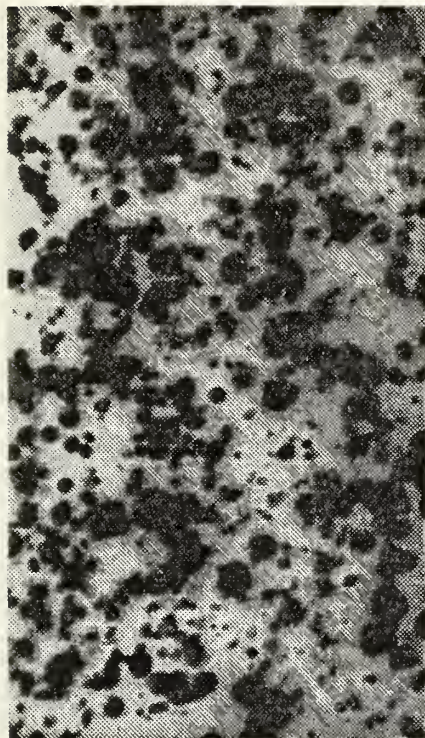


(c)

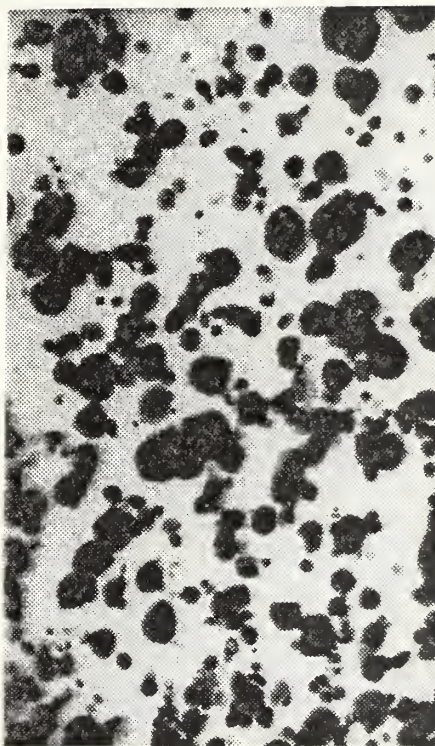
Figure 20. Carbon Extraction Micrograph of Treatment-D (prior to rolling): (a) Magnification 5,000X; (b) Magnification 10,000X; (c) Magnification 15,000X. Structure shows distribution of carbides.



(a)

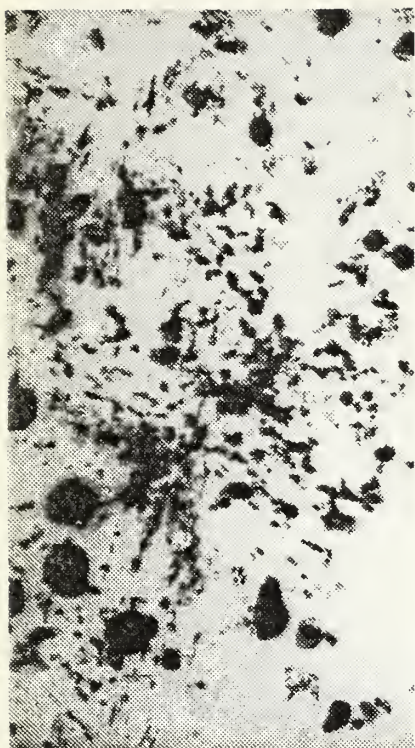


(b)



(c)

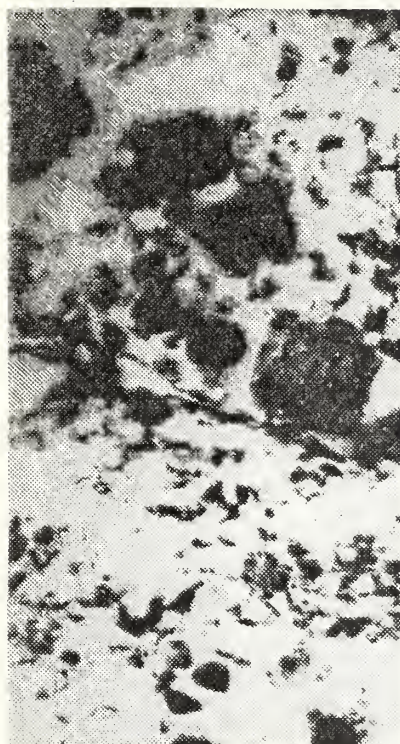
Figure 21. Carbon Extraction Micrograph of Treatment-D (as rolled): (a) Magnification 5,000X; (b) Magnification 10,000X; (c) Magnification 15,000X. Structure shows distribution of carbides.



(a)

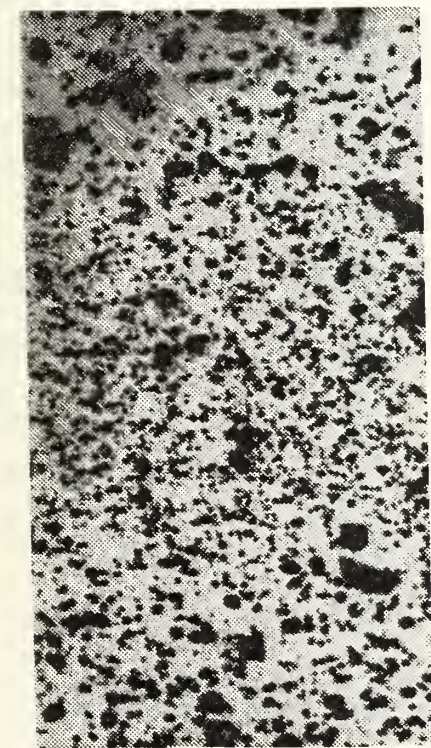


(b)

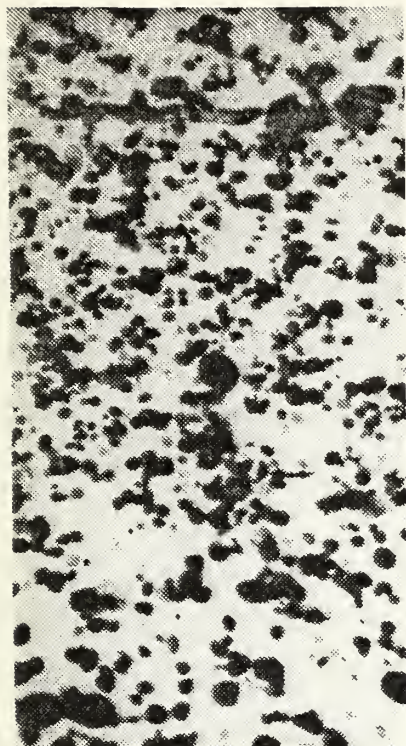


(c)

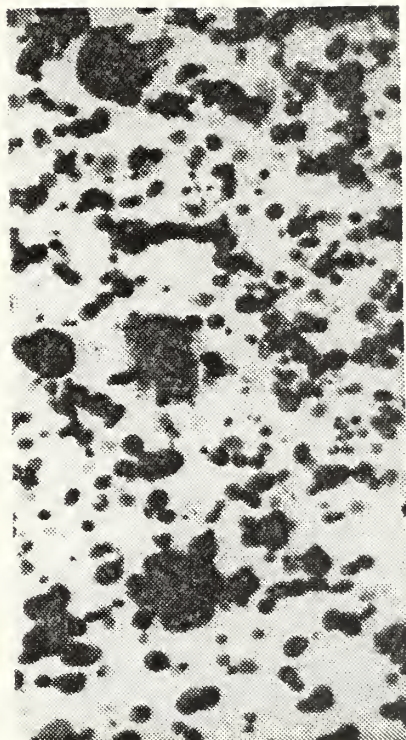
Figure 22. Carbon Extraction Micrograph of Treatment-B (prior to rolling): (a) Magnification 5,000X; (b) Magnification 10,000X; (c) Magnification 15,000X. Structure shows distribution of carbides.



(a)



(b)



(c)

Figure 23. Carbon Extraction Micrograph of Treatment-E (as rolled): (a) Magnification 5,000X; (b) Magnification 10,000X; (c) Magnification 15,000X. Structure shows distribution of carbides.

of the original carbides, the resulting microstructures are banded and contain remnants of the as-normalized pearlitic structure. The degree of solutioning of the carbides is a function of austenitizing temperature and time, higher temperatures and longer times producing fewer residual carbides. Experimentally, the 1000 degree Celsius austenitizing temperature processes (treatments B and D) have fewer residual carbides than the 850 degree Celsius austenitizing temperature processes (treatments A, C, and E).

The mechanical properties of the as thermo-mechanically treated material show no significant difference between the four treatments except the lack of work hardening observed in treatments C, D, and E. However, a significant increase in the yield strength is realized through all the thermo-mechanical treatments when compared to the normalized structure of the standard bearing heat treatment (treatment-A).

B. HARDENING RESPONSE OF AS TREATED MATERIAL

1. Mechanical Test Results

Mechanical testing was conducted on the as-rolled conditions of treatments A through E. Specimens of each treatment were then austenitized at three austenitizing temperatures for times ranging from five minutes to sixty minutes, and subsequently quenched in warm oil (50 degrees Celsius). Rockwell-C hardness readings were taken at each time for each of the three austenitizing temperatures. The results are plotted for treatments A through E and Figures 24 through 28

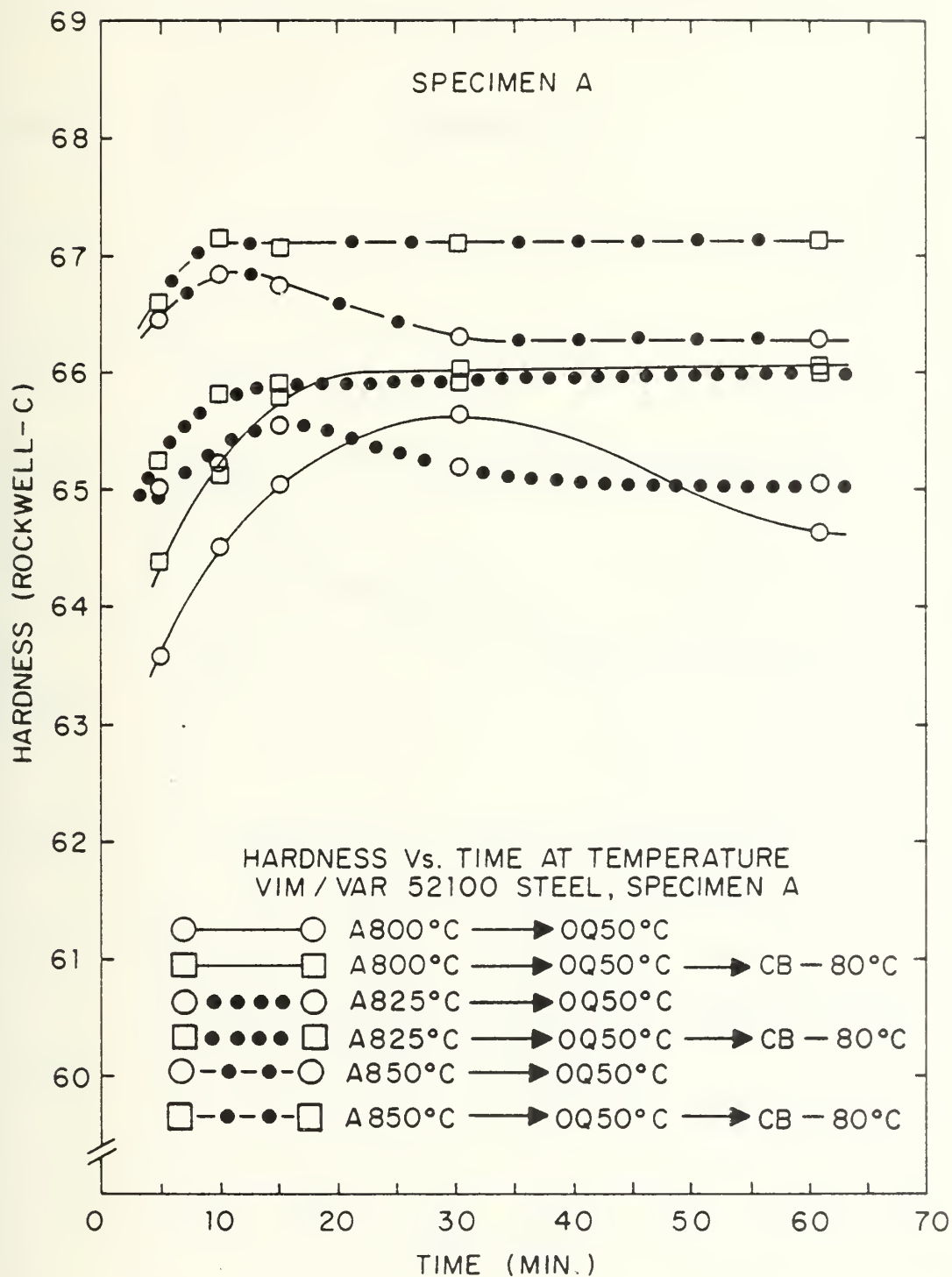


Figure 24. Hardening Response of Treatment-A

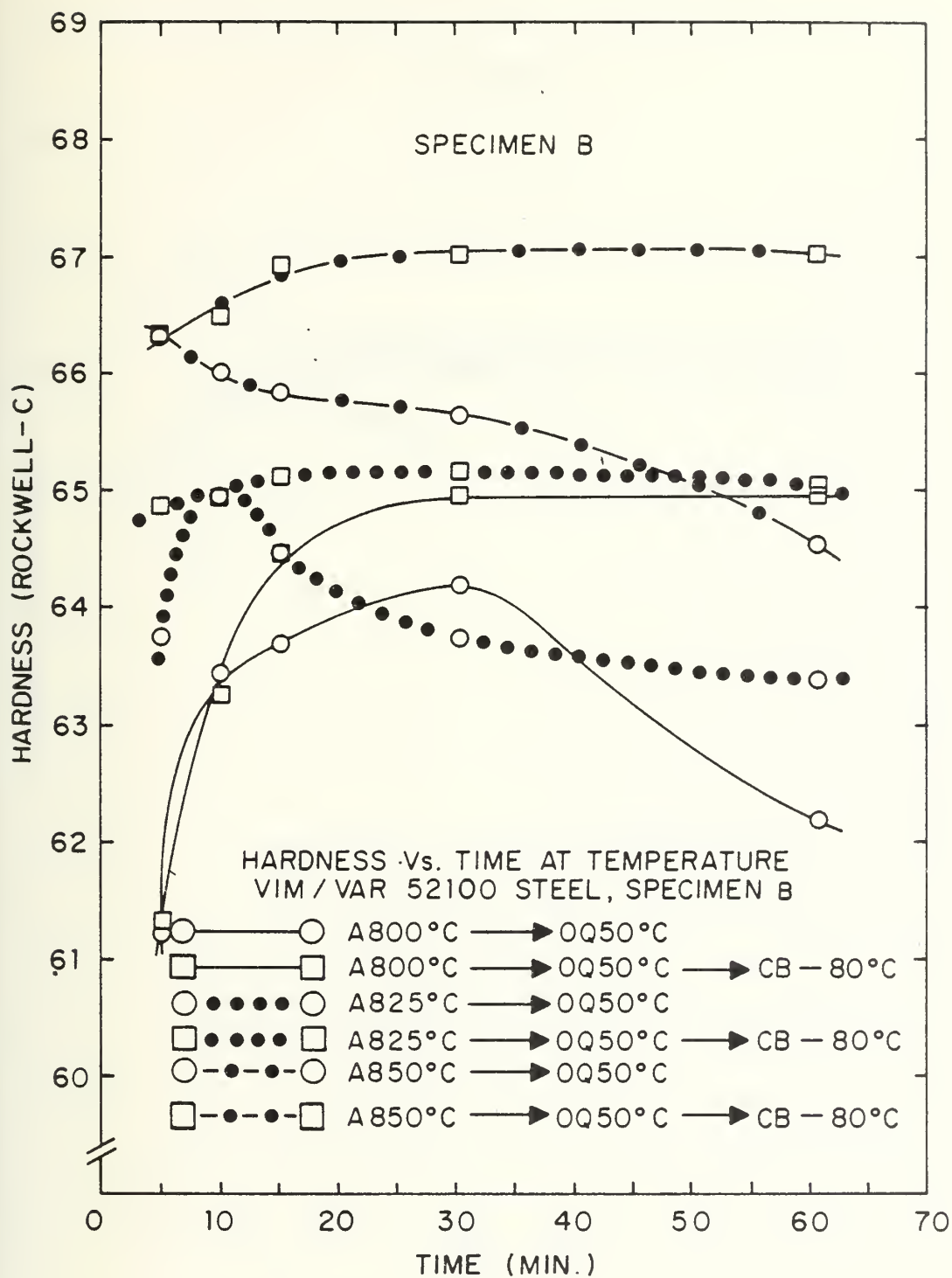


Figure 25. Hardening Response of Treatment-B

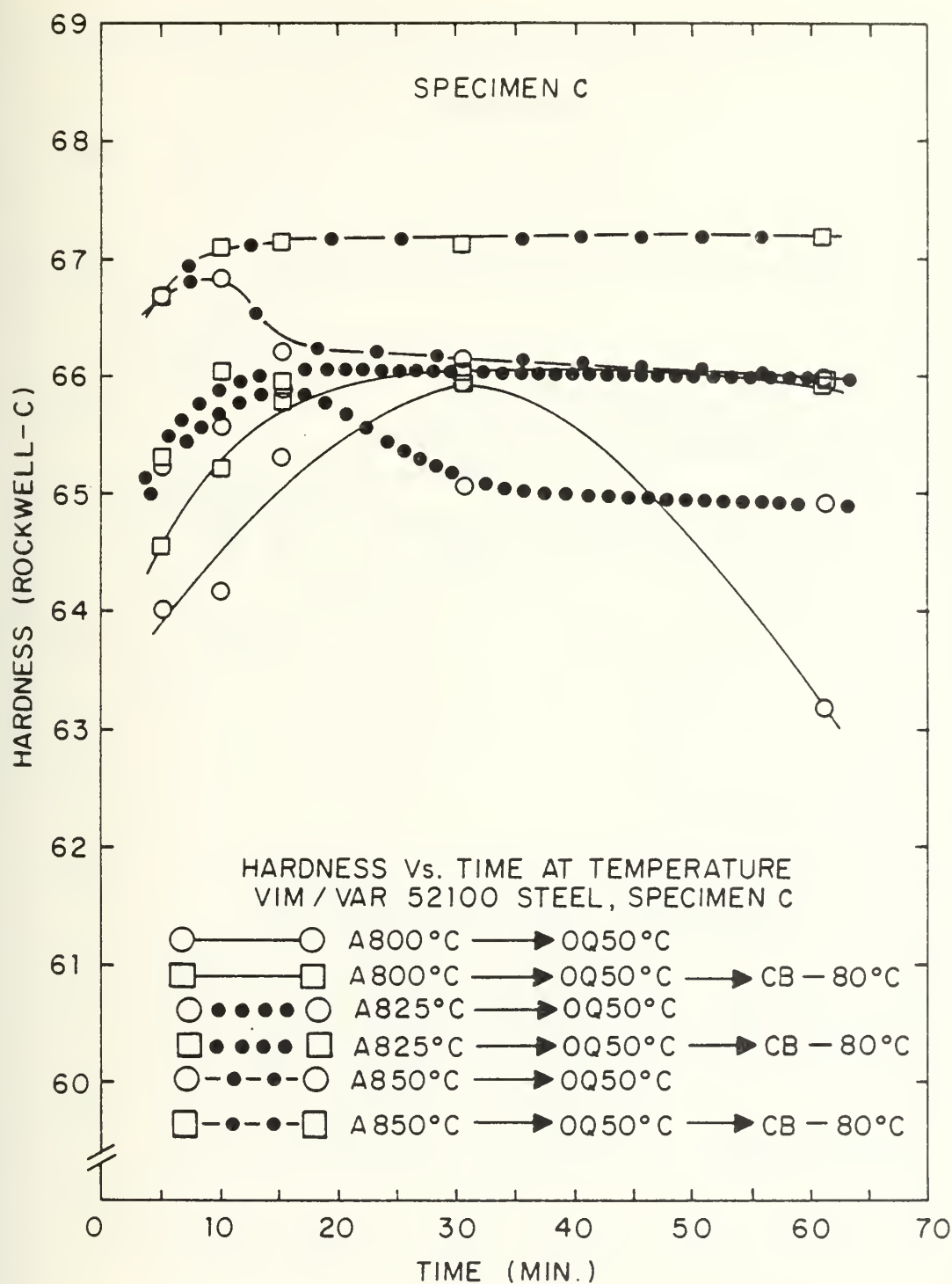


Figure 26. Hardening Response of Treatment-C

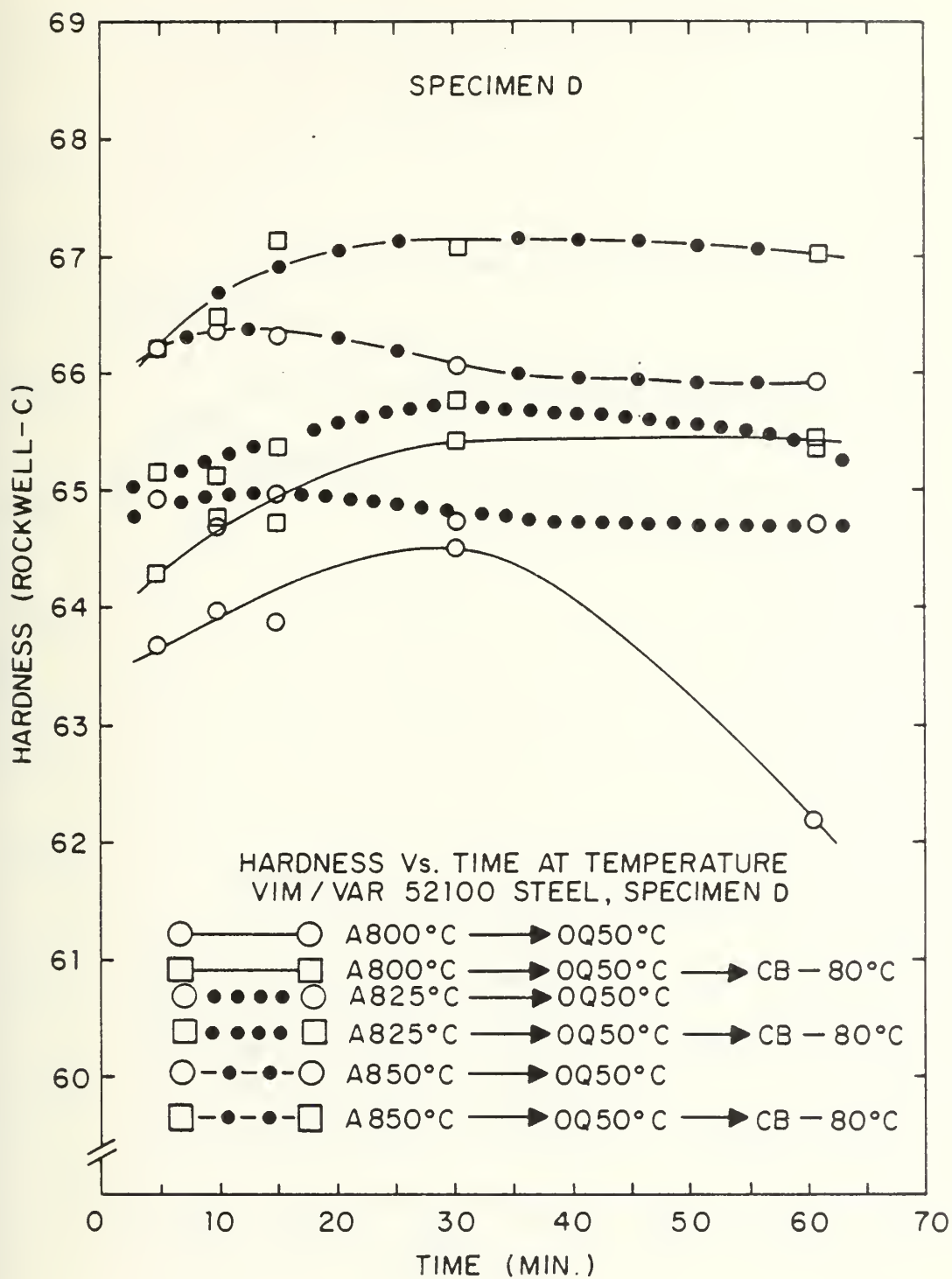


Figure 27. Hardening Response to Treatment-D

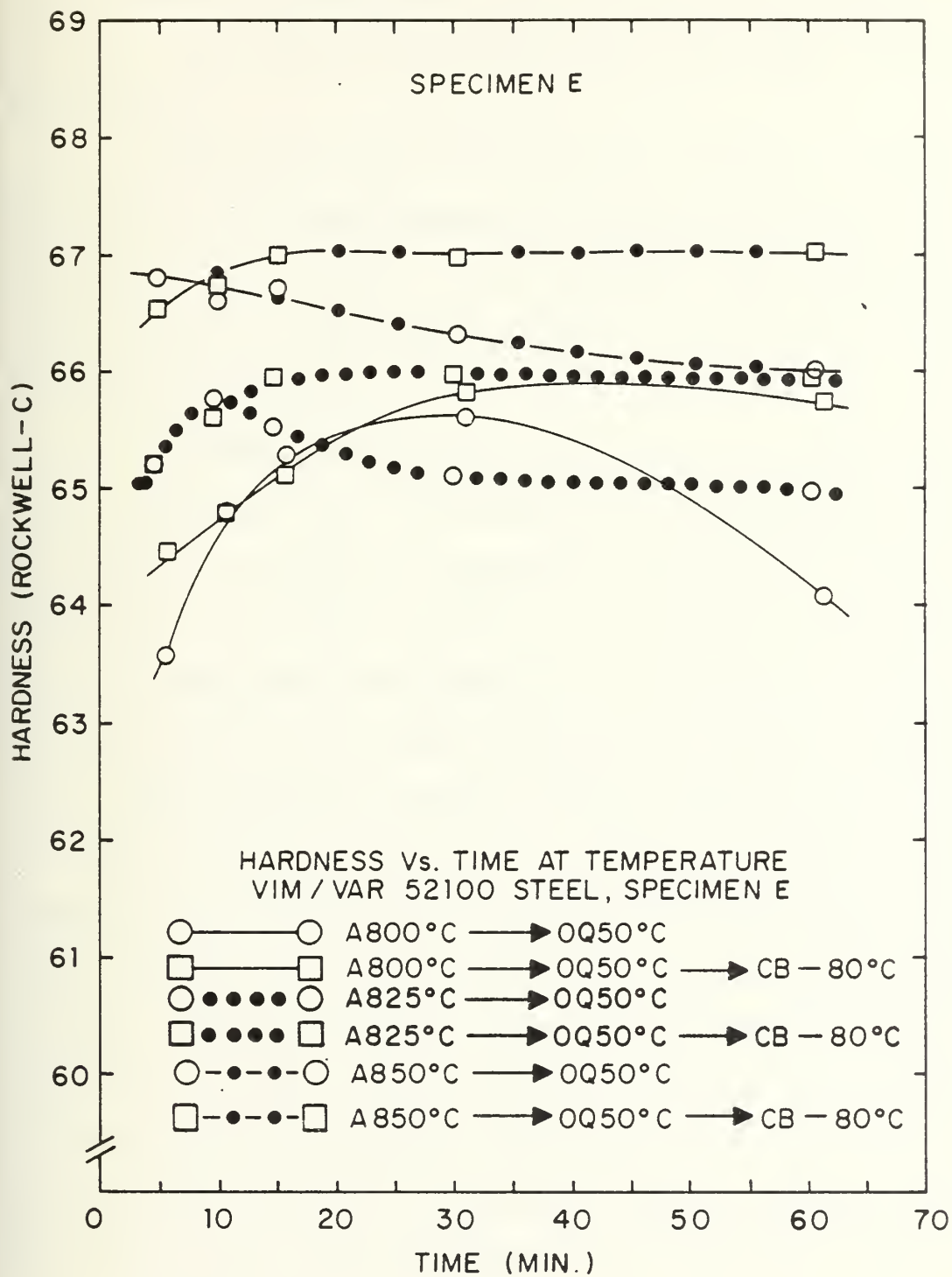


Figure 28. Hardening Response of Treatment-E

respectively. Generally, the as quenched hardness increased as the time at temperature increased until a maximum was realized. As the time increased past this peak, the hardness decreased.

As austenitizing temperature increased, the time required to achieve peak hardness decreased and the peak hardness increased. This effect is most apparent when comparing the curves resulting from austenitizing at 850 degrees Celsius and 825 degrees Celsius.

In order to determine the effect of retained austenite, X-ray techniques [Ref. 24] were used to determine the amount of retained austenite in specimens from groups A and B. These results are tabulated in Table 3. Additionally, specimens from all groups were refrigerated to -80 degrees Celsius to show the effect of retained austenite on the as quenched hardness. The difference between the room temperature hardness and the refrigerated hardness is indicative of this effect. Generally, this difference is greater for specimens austenitized at 850 degrees Celsius than for those at 825 degrees Celsius. Additionally, the thermo-mechanically treated materials (B through E) have greater differences than the unrolled, standard material (treatment-A). This is in agreement with Table 3, which shows greater percent retained austenite in the rolled specimens and this value increases as the temperature is increased. Also, these results are in agreement with Stickels' results [Ref. 21], which indicate

that the quantity of retained increases as the austenitizing temperature increases and as the grain size decreases.

Table 3. RETAINED AUSTENITE DETERMINATION

TREATMENT	TEMPERATURE DEGREES C	TIME MINUTES	PERCENT RETAINED AUSTENITE
A	800	5	trace
A	800	15	1.0
A	800	60	1.0
A	825	5	trace
A	825	15	2.1
A	825	60	2.4
A	850	5	4.5
A	850	15	5.2
A	850	60	8.6
B	800	5	2.3
B	800	15	5.0
B	800	60	7.0
B	825	5	5.0
B	825	15	8.8
B	825	60	11.3
B	850	5	8.6
B	850	15	10.0
B	850	60	12.9

The curves for the 800 degrees Celsius austenitizing temperature do not correlate with the measured results in Table 3, nor do they agree with the trends reported by Stickels and supported by the curves for the 825 and 850 degrees Celsius austenitizing temperatures. There are two possible explanations for this unusual effect: (1) at 800 degrees Celsius the carbon content of the retained austenite is higher than that at 825 and 850 degrees Celsius which, when transformed to martensite at -80 degrees Celsius, produces a martensite of higher hardness

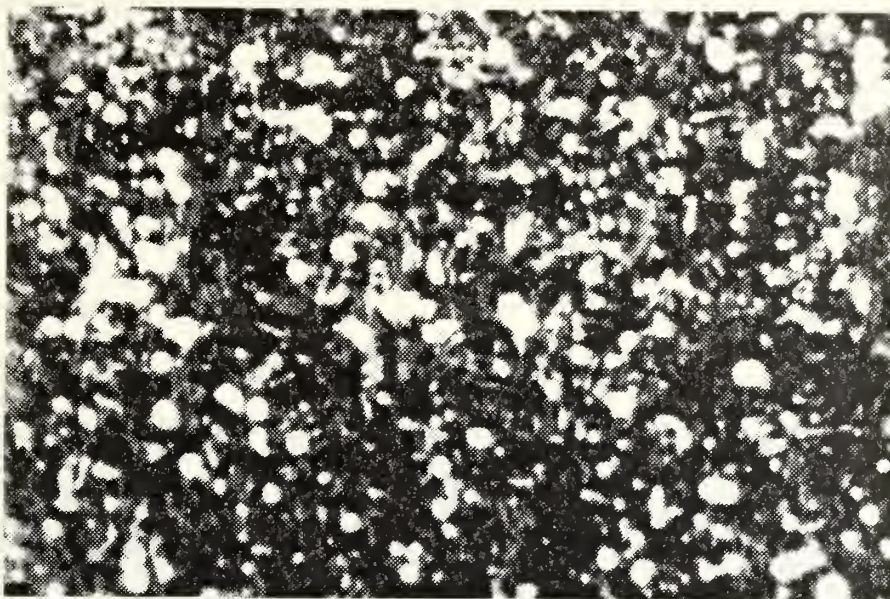


Figure 29a

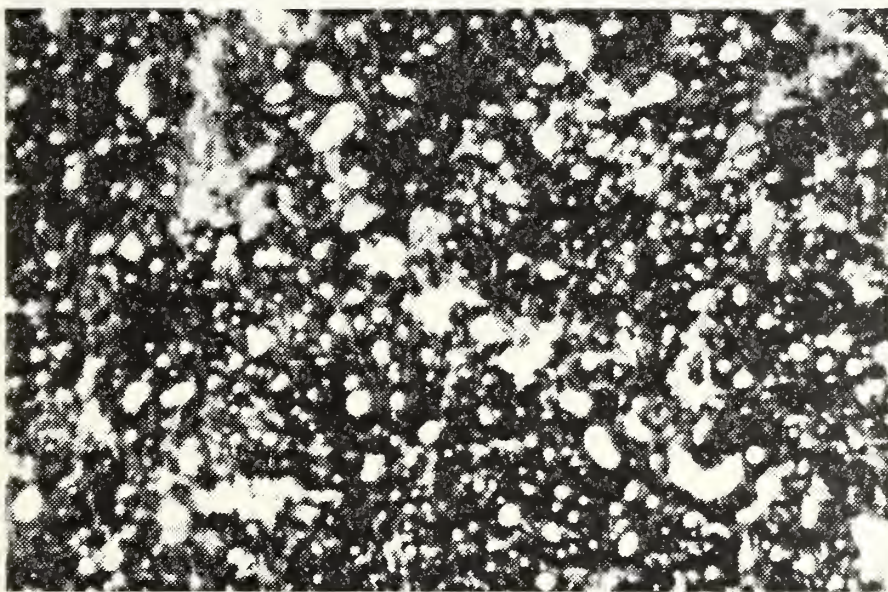


Figure 29b

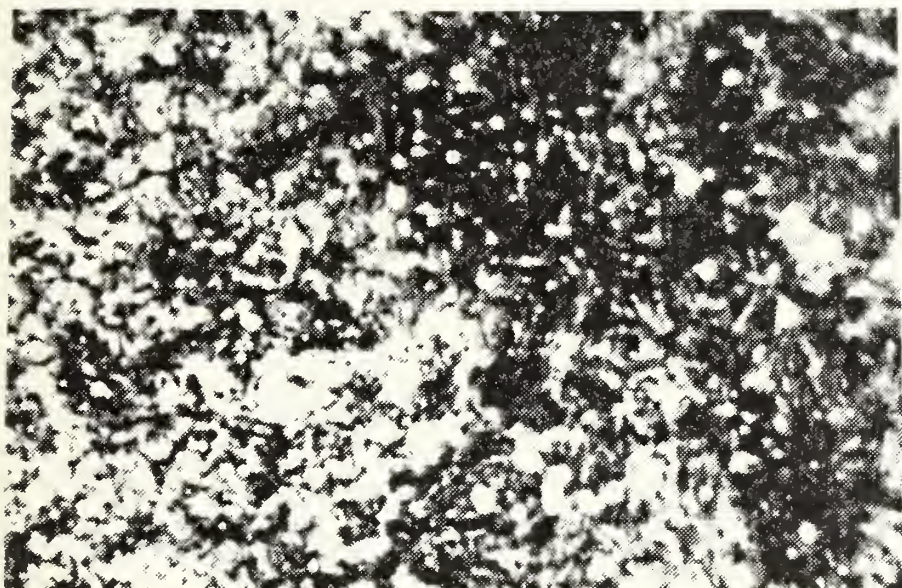


Figure 29c

Figure 29. Optical Micrographs of Hardened AISI 52100 Steel: (a) Treatment-A austenitized 850 degrees Celsius for 60 minutes then oil quenched, (b) Treatment-B austenitized 850 degrees Celsius for 60 minutes then oil quenched, and (c) Treatment-C austenitized 850 degrees Celsius for 60 minutes then oil quenched. Magnification 1000X.

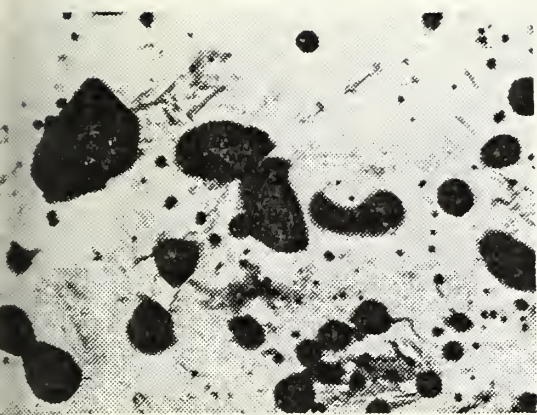
thus exhibiting a larger increase, and (2) the 800 degrees Celsius martensite produced upon refrigeration has a much finer crystalline structure than that produced at the higher austenitizing temperatures, thus resulting in a larger increase in hardness. Either of these two explanations or both in combination would result in the observed effects at 800 degrees Celsius.

2. Microstructural Results

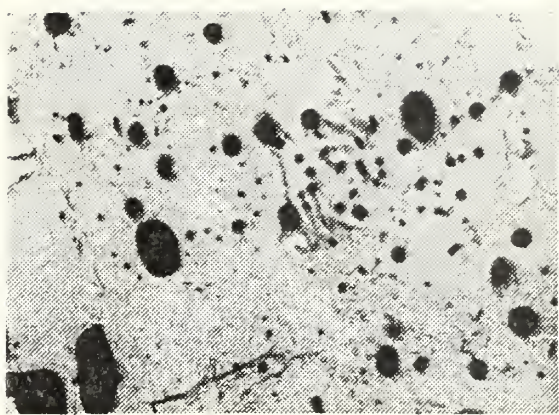
Optical microscopy was conducted on specimens from each of the thermo-mechanical treatment groups at each temperature for austenitizing times of 5, 15, and 60 minutes. Optical micrographs of specimens from treatment groups A, B, and C, austenitized at 850 degrees Celsius for 60 minutes are shown in Figure 29. The structure is too fine to obtain any detailed structural information other than an indication of residual carbide size and distribution, with the exception of specimen B which still shows indication of the banding from the as rolled structure.

Carbon extraction replicas were obtained from the specimens of treatments A, B, and C, austenitized at 825 and 850 degrees Celsius for 5, 15, and 60 minutes. These micrographs are shown in Figures 30 through 35, and show the response of the carbides with increasing time at austenitizing temperatures.

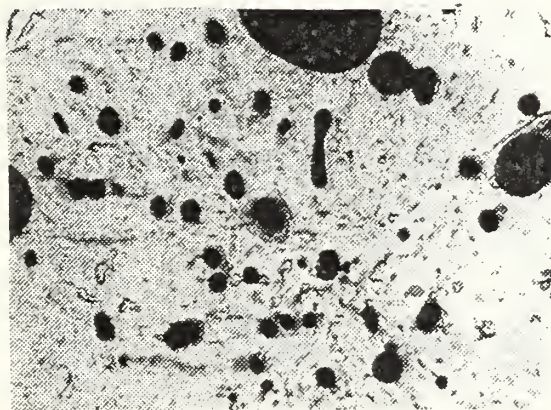
At the 825 degree Celsius austenitizing temperature the specimens from treatment-A indicated initial carbide



(a)

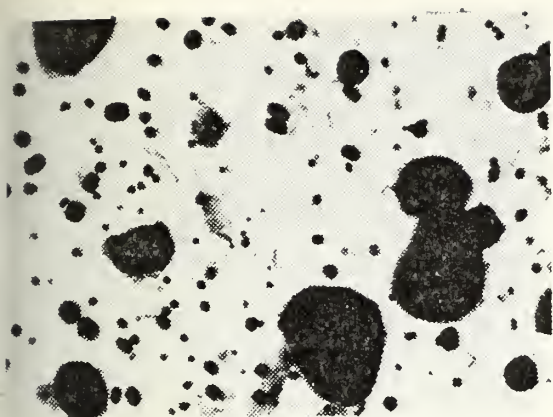


(b)

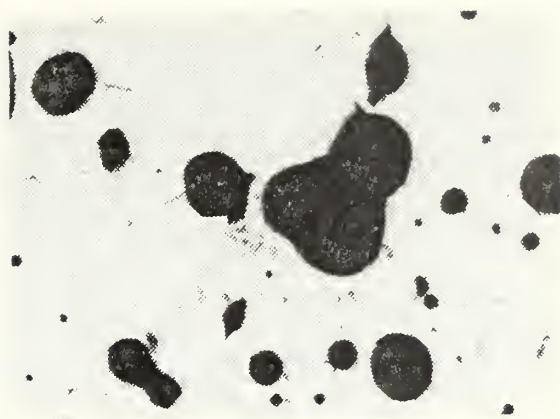


(c)

Figure 30. Carbon Extraction Replica of Treatment-A Austenitized at 825 degrees Celsius: (a) austenitized 5 minutes, (b) austenitized 15 minutes, and (c) austenitized 60 minutes. Micrographs show response of carbides to time at austenitizing temperature. Magnification 10,000X.



(a)

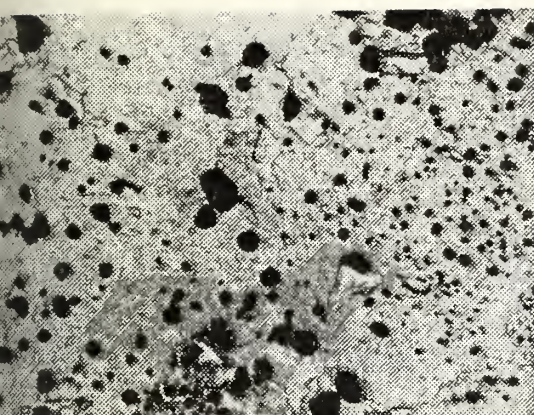


(b)

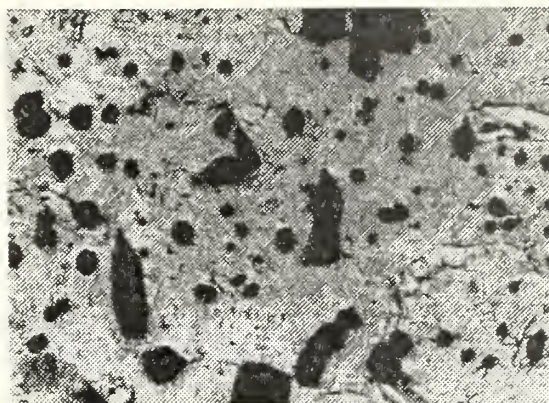


(c)

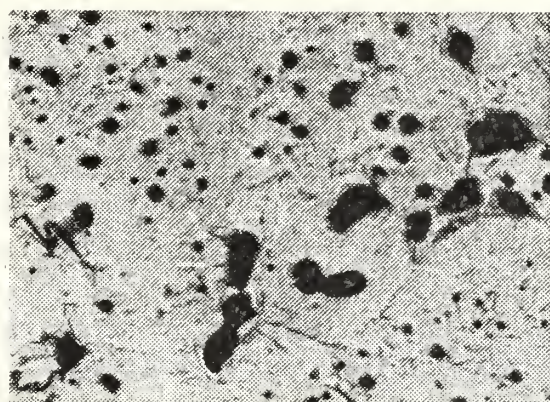
Figure 31. Carbon Extraction Replica of Treatment-A Austenitized at 850 degrees Celsius: (a) austenitized 5 minutes, (b) austenitized 15 minutes, and (c) austenitized 60 minutes. Micrograph shows response of carbides to time at austenitizing temperature. Magnification 10,000X.



(a)



(b)



(c)

Figure 32. Carbon Extraction Replica of Treatment-B Austenitized at 825 degrees Celsius: (a) austenitized 5 minutes, (b) austenitized 15 minutes, and (c) austenitized 60 minutes. Micrographs show response of carbides to time at austenitizing temperature. Note presence of banding. Magnification 10,000X.

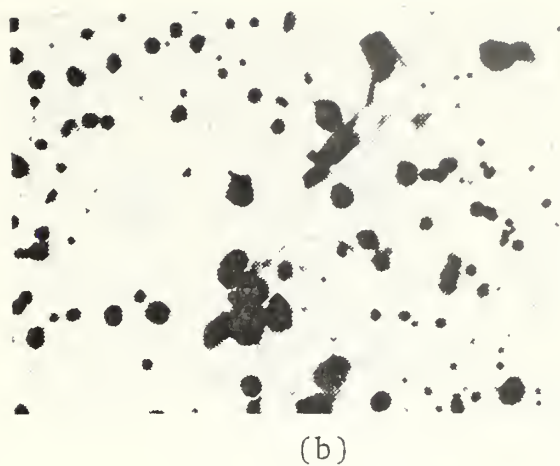
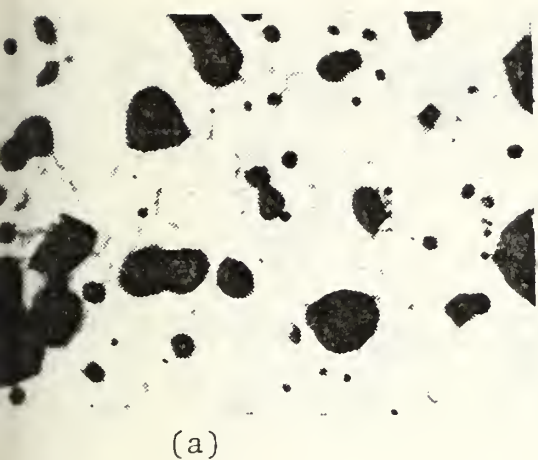
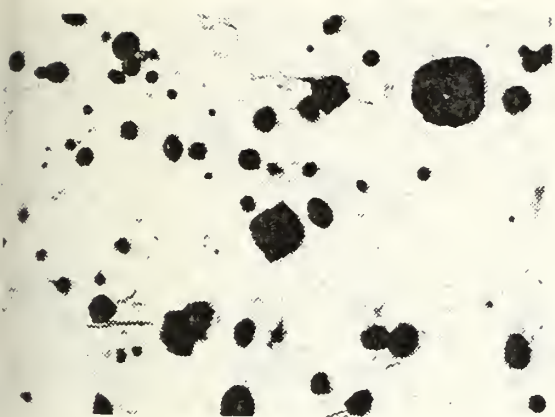
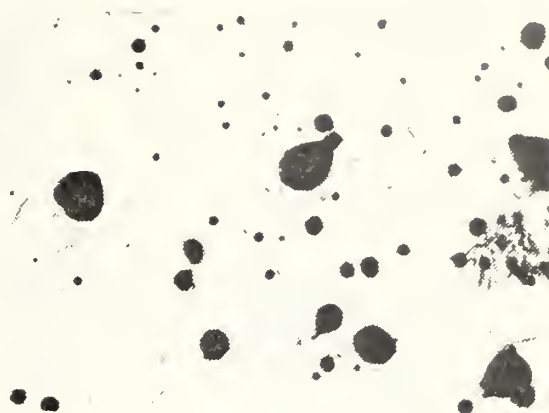


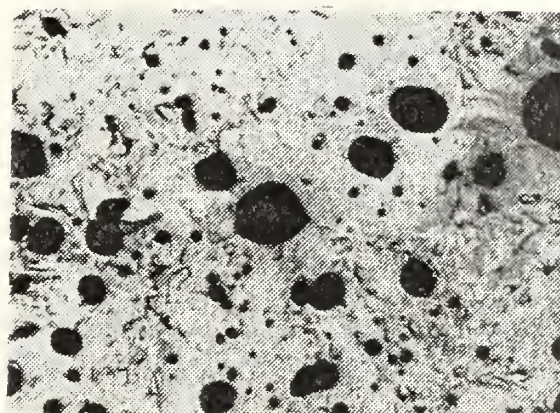
Figure 33. Carbon Extraction Replica of Treatment-B Austenitized at 850 degrees Celsius: (a) austenitized 5 minutes, (b) austenitized 15 minutes, and (c) austenitized 60 minutes. Micrographs show response of carbides to time at austenitizing temperature. Note banding in structure. Magnification 10,000X.



(a)



(b)

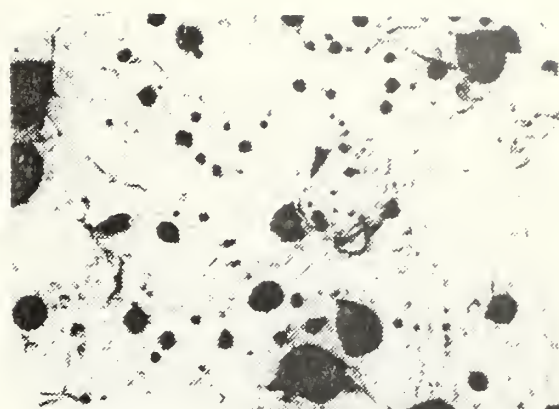


(c)

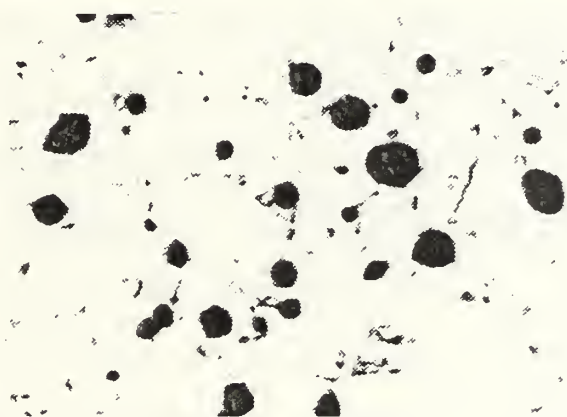
Figure 34. Carbon Extraction Replica of Treatment-C Austenitized at 825 degrees Celsius: (a) austenitized 5 minutes, (b) austenitized 15 minutes, and (c) austenitized 60 minutes. Micrograph shows response of carbides to time at austenitizing temperature. Magnification 10,000X.



(a)



(b)



(c)

Figure 35. Carbon Extraction Replica of Treatment-C Austenitized at 850 degrees Celsius: (a) austenitized 5 minutes, (b) austenitized 15 minutes, and (c) austenitized 60 minutes. Micrograph shows response of carbides to time at austenitizing temperature. Magnification 10,000X.

size after 5 minutes at temperature, ranging from less than 0.1 microns up to a maximum of 2.5 microns. As the time at temperature was increased, the size of the residual carbides decreased only slightly, but the carbide density decreased significantly. The dissolution of the smaller carbides is the primary contributor to this decrease. As the carbide density decreases the carbon content of the matrix increases, increasing the hardness and retained austenite content up to a maximum. This accounts for the flattening that occurs in the refrigerated hardness curves. At 850 degrees Celsius temperature, the dissolution of the carbides occurs faster as is evident in the carbon extraction micrographs. Also evident in the micrographs is the coarsening that is occurring in the carbide structure, which was also observed by Stickels [Ref. 21]. In this series, quench cracking was observed in all specimens austenitized at 850 degrees Celsius for time of greater than 10 minutes. Austenitizing at 825 degrees Celsius did not result in cracking at times up to 60 minutes in treatment-A specimens or in any other treatment group.

Treatment-B specimens exhibited a slightly different response in that dissolution and coarsening appear to be occurring at a faster rate in the 825 degree Celsius treatment than in the same austenitizing treatment in the treatment-A group. Examination of the microstructures of specimens hardened for 15 minutes and 60 minutes, both at 825 degrees Celsius and 850 degrees Celsius, show few changes in structure.

As in the treatment-A group, quench cracking was observed at times greater than 10 minutes at the 850 degree Celsius austenitizing temperature.

Treatment-C's response to increases in time at austenitizing temperatures is somewhat similar to that observed for the A and B treatment group. However, the lack of the smaller carbides at the 5 minute austenitizing time when compared to the as-rolled structure indicates that the dissolution rate is faster in this treatment group at both the 825 and 850 degree Celsius austenitizing temperature. Also it appears that coarsening is still occurring at 60 minutes in the 825 degree Celsius treatment, while at the 850 degree Celsius austenitizing temperature the lack of change of microstructure with time at times of 15 minutes and more mentioned in the discussion of the treatment-B results is evident. The quench cracking observed in the A and B treatment groups was not evident in the treatment-C specimens at times up to and including 60 minutes.

Microscopic examination of the treatment D and E groups revealed that quench cracking occurred in the D group at time of greater than 10 minutes at an austenitizing temperature of 850 degrees Celsius, whereas treatment-E specimens, like treatment-C specimens, exhibited no tendency to crack at times up to 60 minutes at 850 degrees Celsius. However, it was observed that all treatment groups exhibited extensive cracking in the specimens refrigerated to -80 degrees Celsius.

3 . Summary of Effects

The response of all treatment groups to hardening at the austenitizing temperatures examined is clearly related to the coarsening and dissolution of the carbides, the as-treated grain size and the carbon content of the austenite prior to quenching. Also, the ultrafine grain structure of the thermo-mechanical treatments accounts for the increased retained austenite content of the as quenched material and the greater increase in hardness when this retained austenite is transformed to martensite by refrigerating the specimens to -80 degrees Celsius. These results are consistent with those obtained by other researchers, in particular the work of Stickels, Ref. [21], and Kar et. al., Ref. [28].

C. TEMPERING RESPONSE OF HARDENED MATERIAL

Based on the results of the hardening response study an austenitizing temperature of 825 degrees Celsius and a time of 15 minutes was chosen to examine the effect of various tempering temperatures on the mechanical properties of hardened AISI 52100 steel subjected to the five treatments (A through E) previously described. Hardness testing was conducted on specimens from each treatment group after tempering times ranging from 0.1 hours to 250 hours at temperatures of 175, 350, and 525 degrees Celsius. Additionally, tensile testing was performed on the specimens from each treatment group after tempering from times ranging

from 10 to 250 hours at temperatures of 350 to 525 degrees Celsius. Tensile testing of 175 degrees Celsius temper was prohibited by the inability effectively to grip specimens of hardnesses greater than 55 Rockwell-C. The results of this testing are plotted for each specimen group in Figures 36 through 45 respectively. Examination of these figures clearly shows that the degradation of mechanical properties with increasing tempering time and temperature is more rapid for the material processed by treatment-A than for the material processed by any of the thermo-mechanical treatments, with treatments C and E being the most resistive to this degradation. No data was obtained for times less than 0.1 hours, so the softening of the material from a hardness of 65 to 50 Rockwell-C at 525 degrees Celsius could not be studied in these experiments.

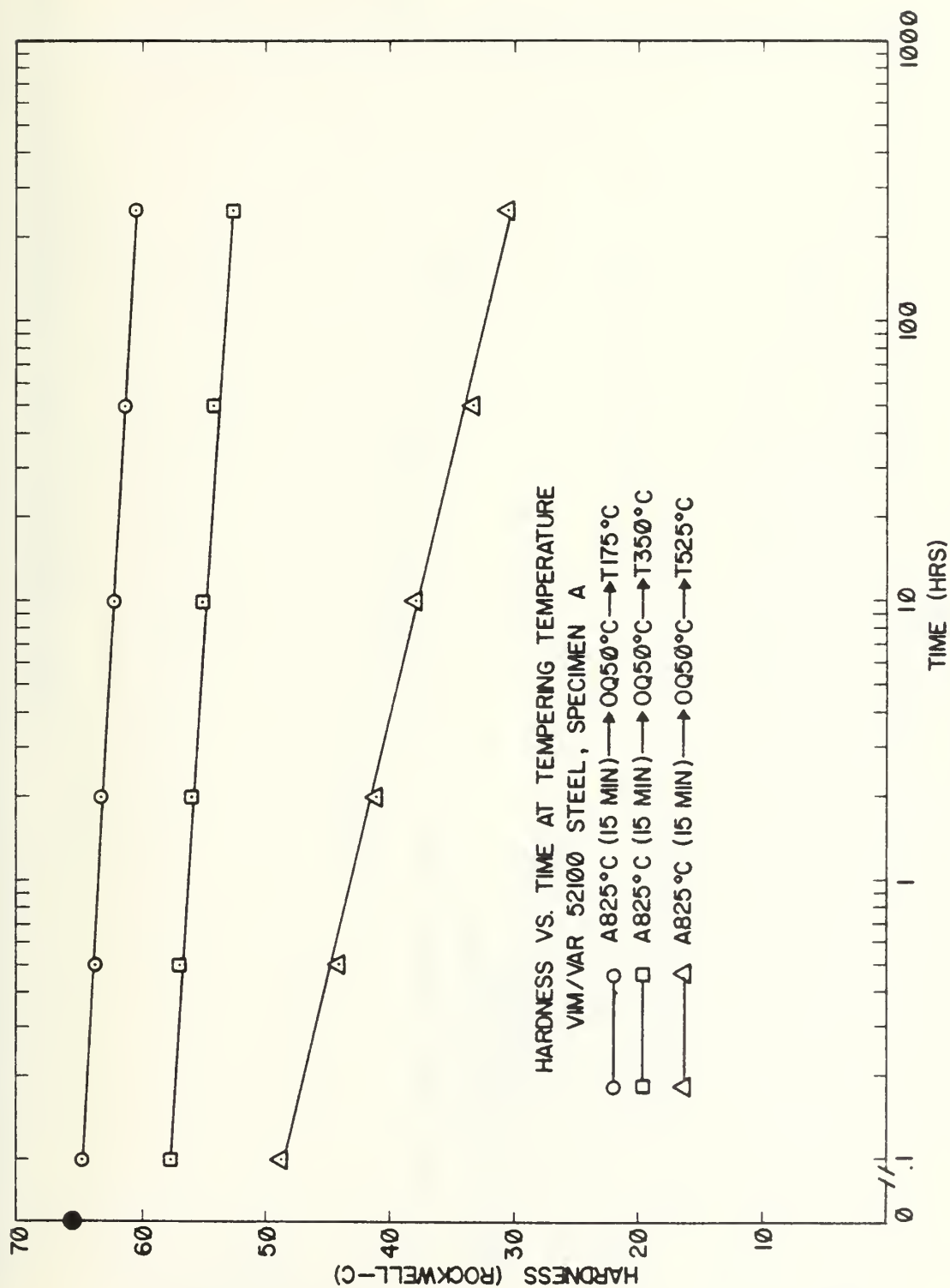


Figure 36. Tempering Response of Treatment-A (Hardness).

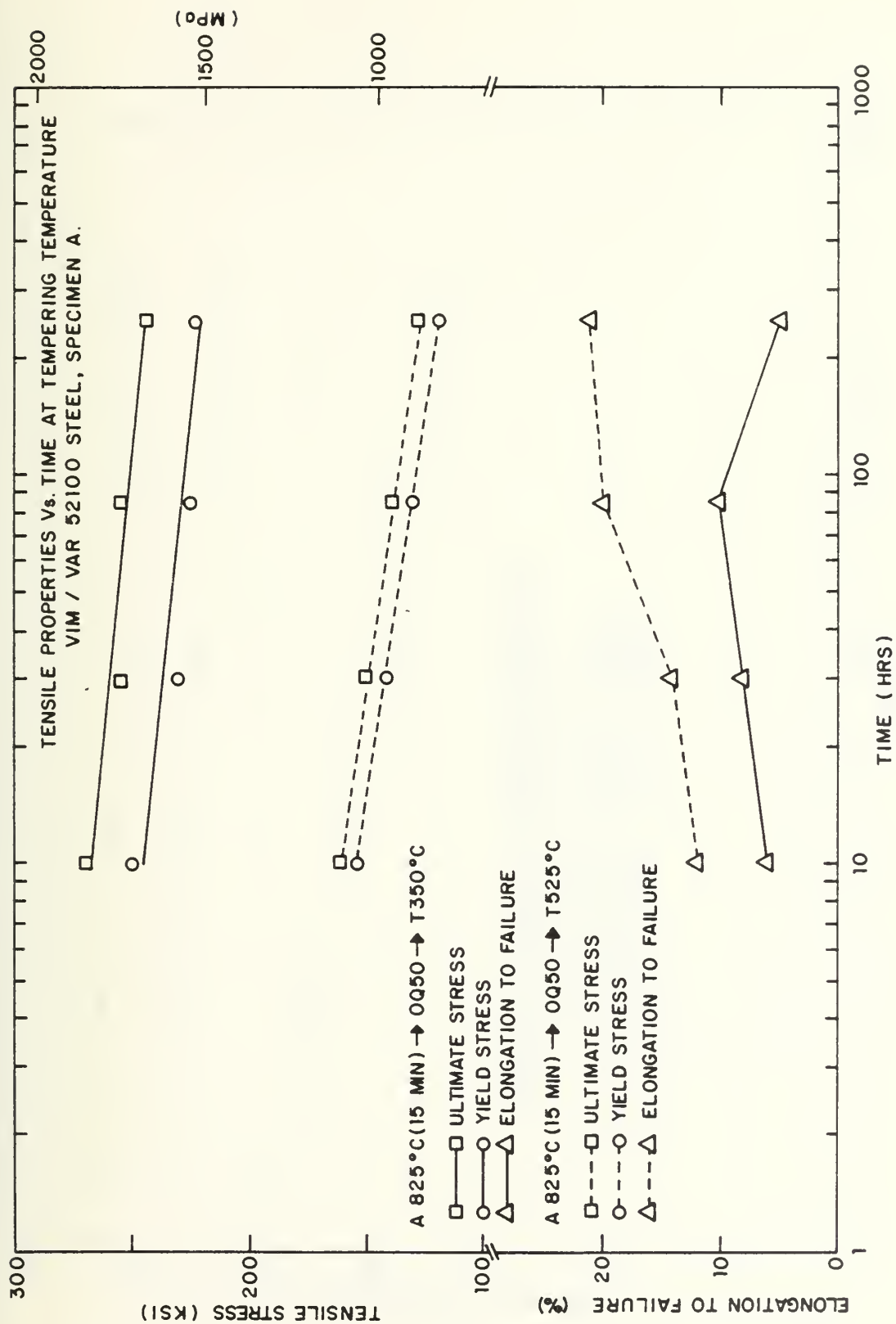


Figure 37. Tempering Response of Treatment-A (Tensile Strength).

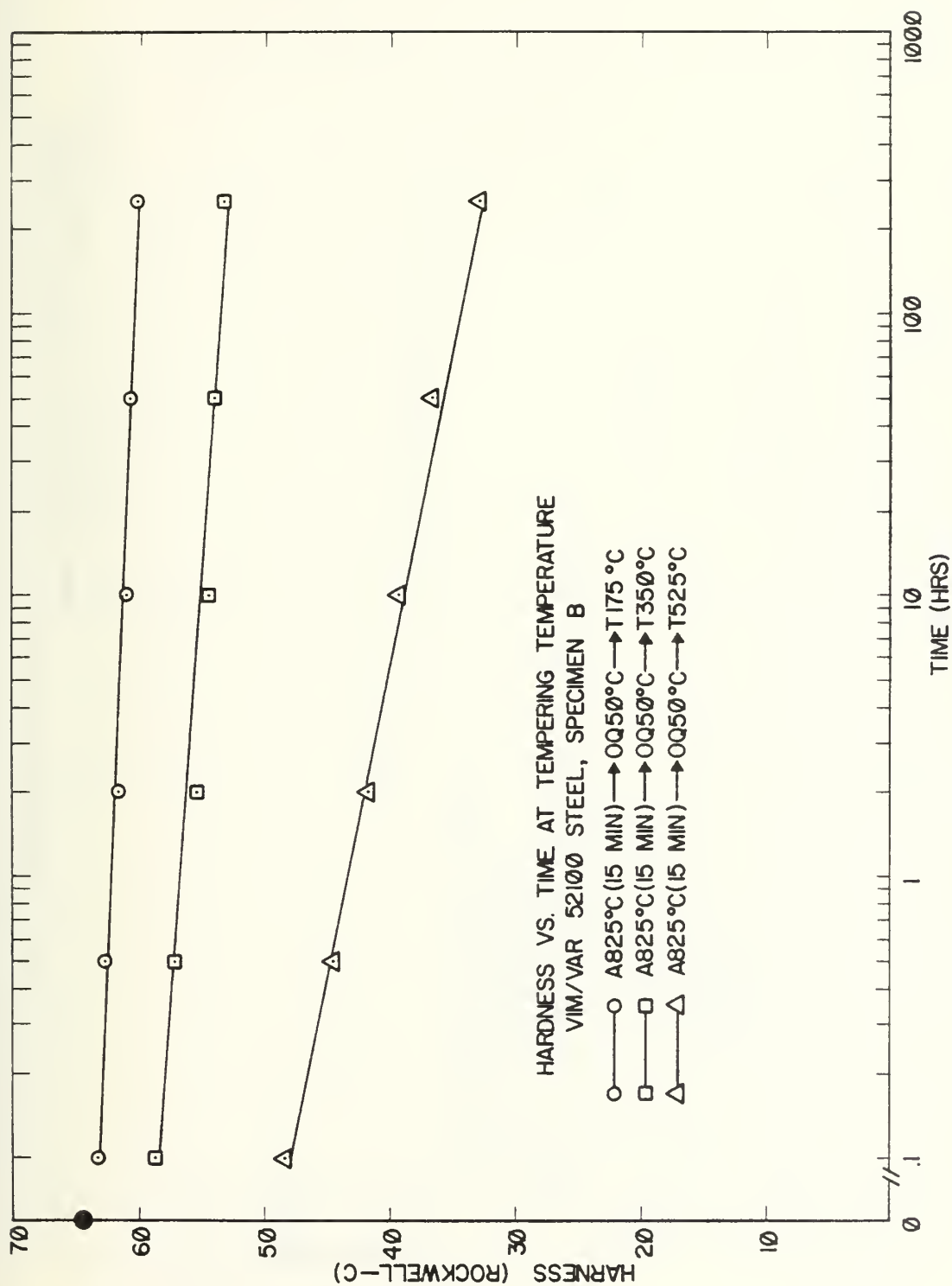


Figure 38. Tempering Response of Treatment-B (Hardness).

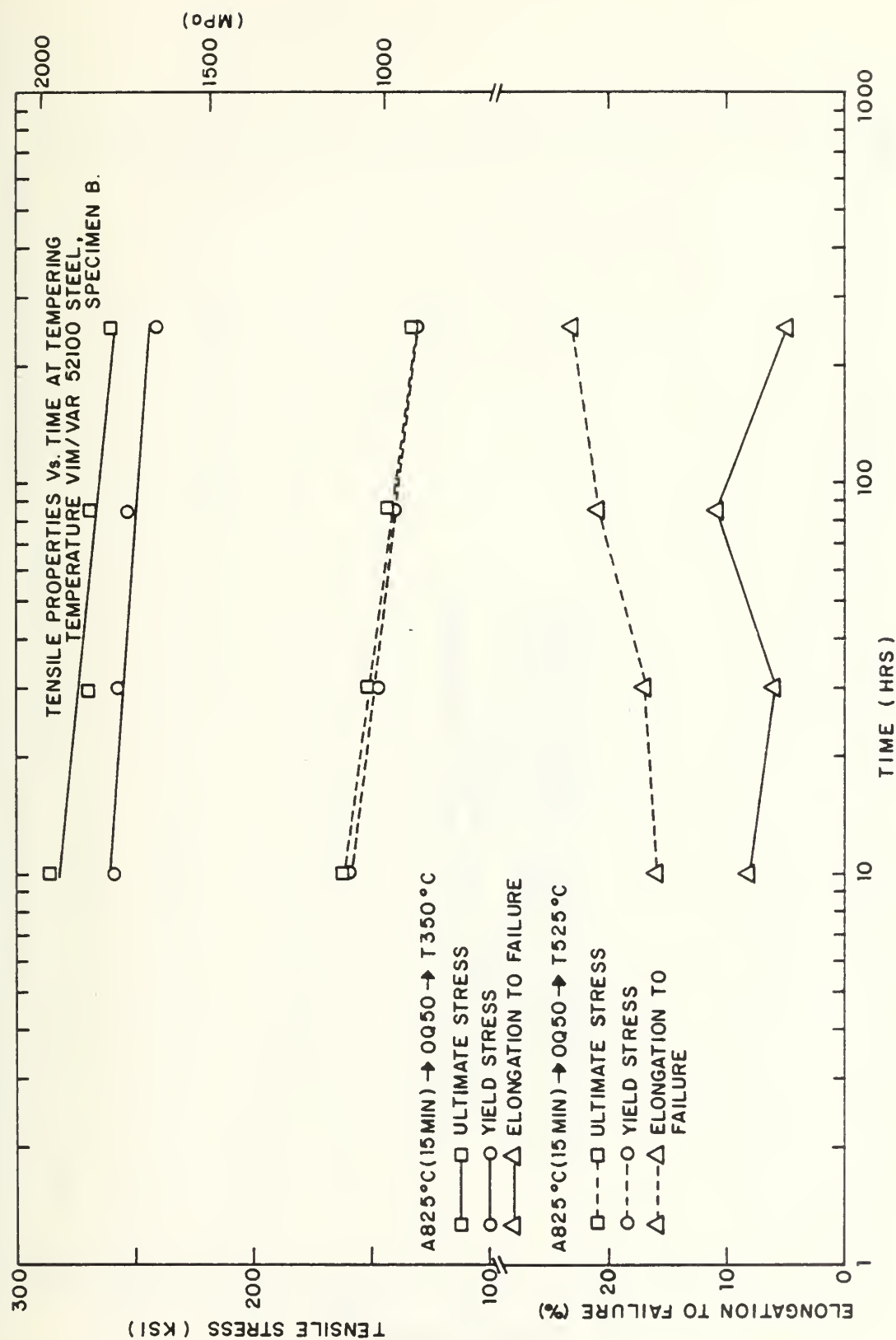


Figure 39. Tempering Response of Treatment-B (Tensile Strength).

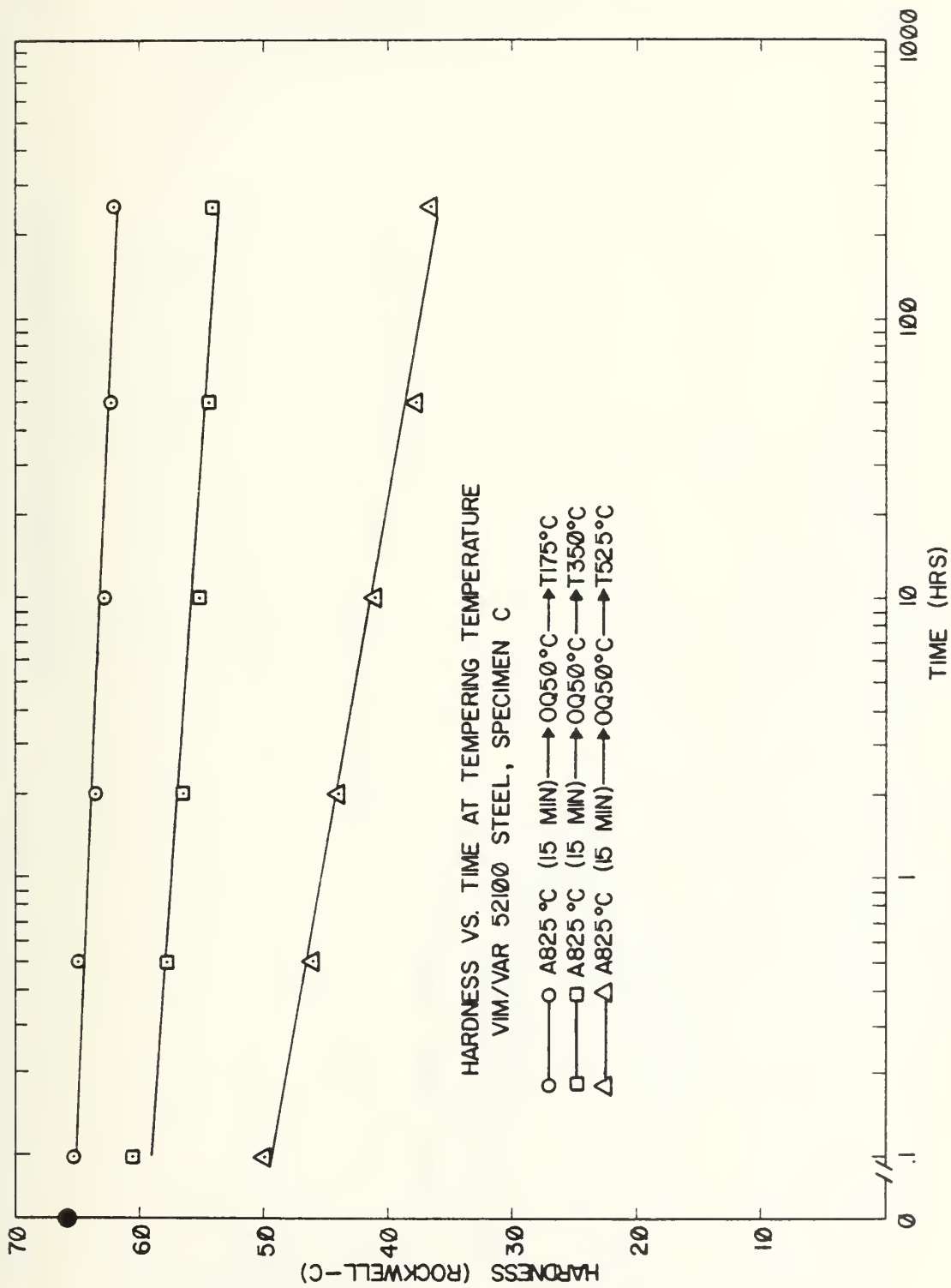


Figure 40. Tempering Response of Treatment-C (Hardness).

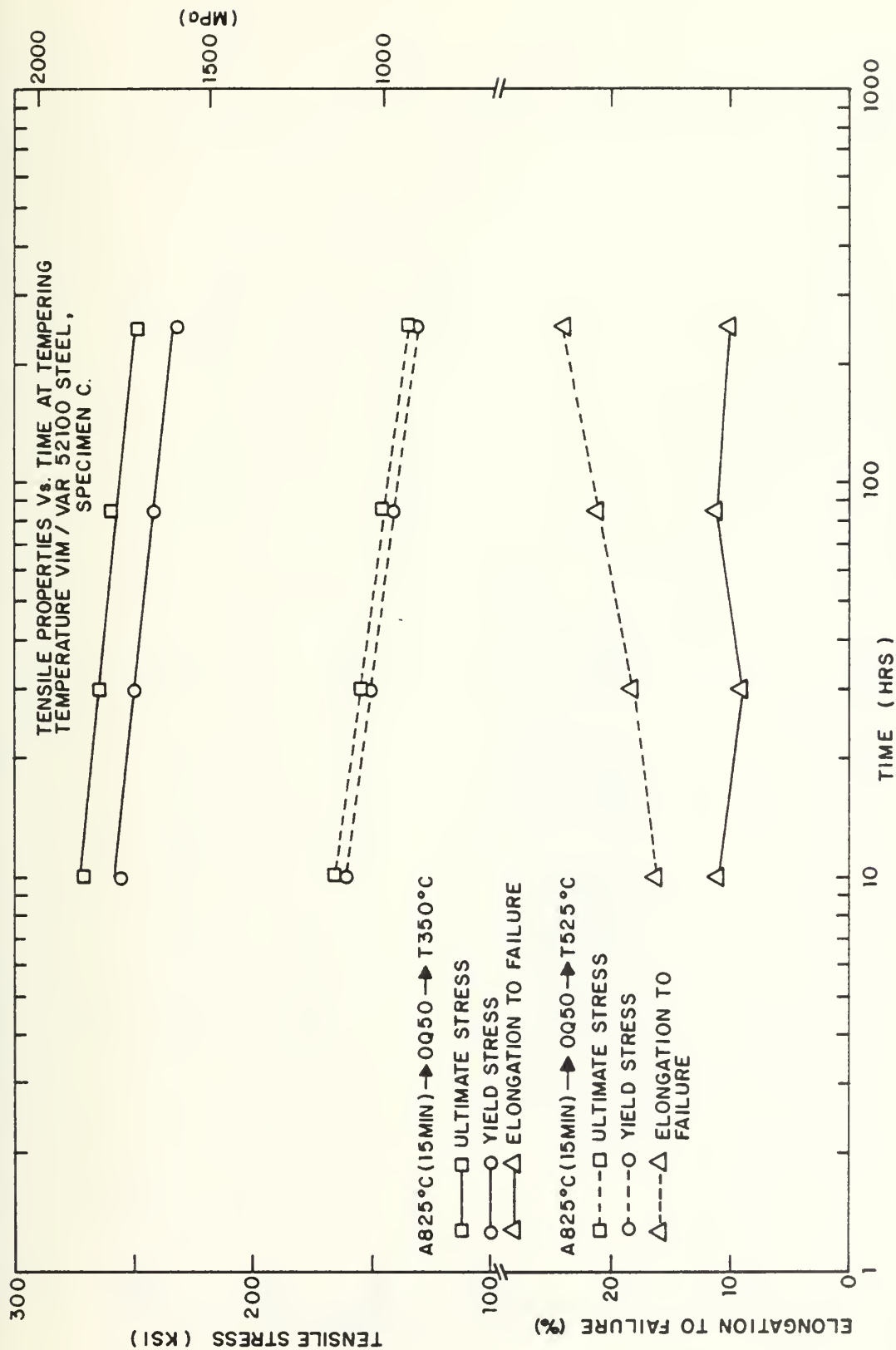


Figure 41. Tempering Response of Treatment-C (Tensile Strength).

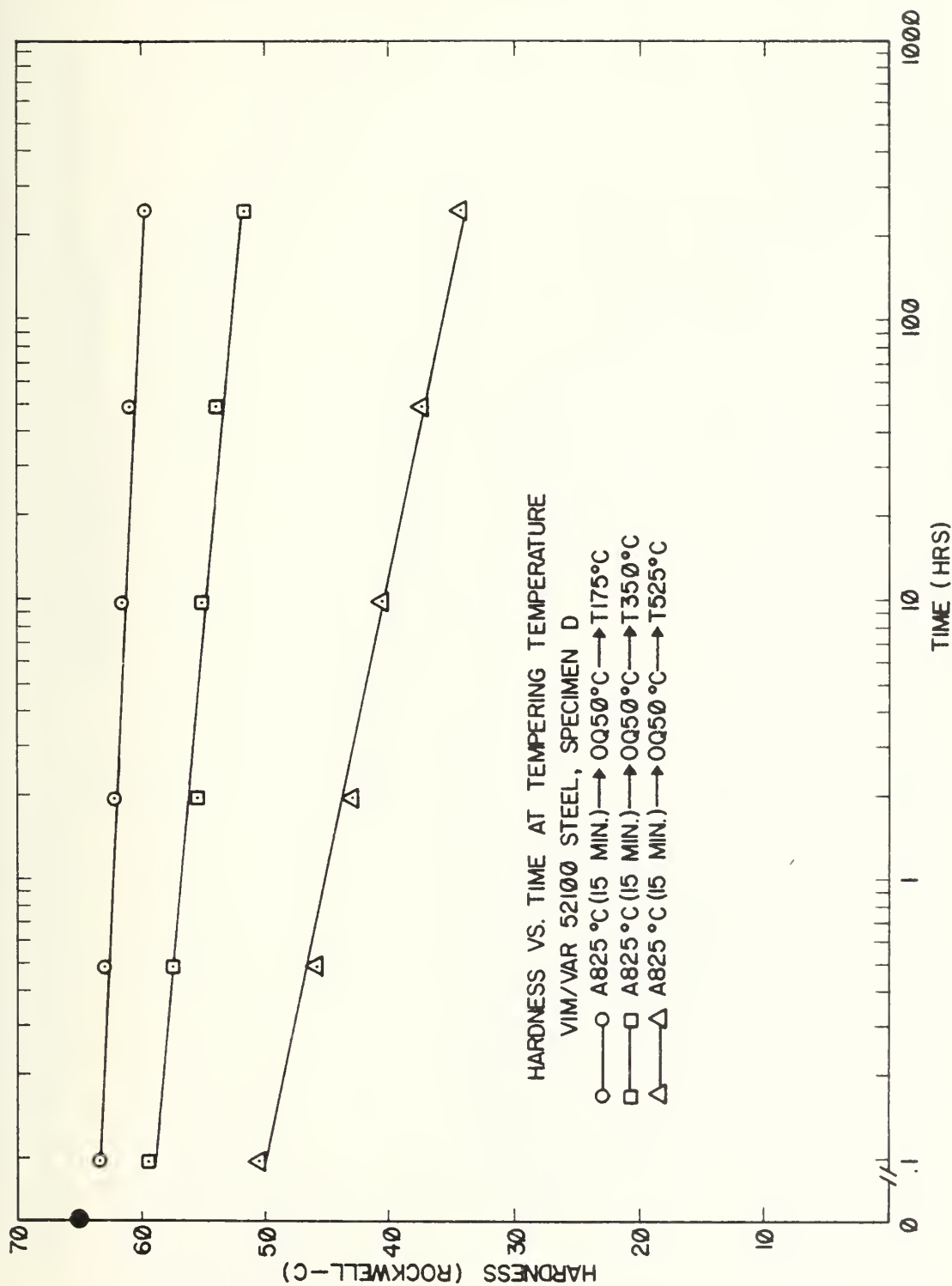


Figure 42. Tempering Response of Treatment-D (Hardness).

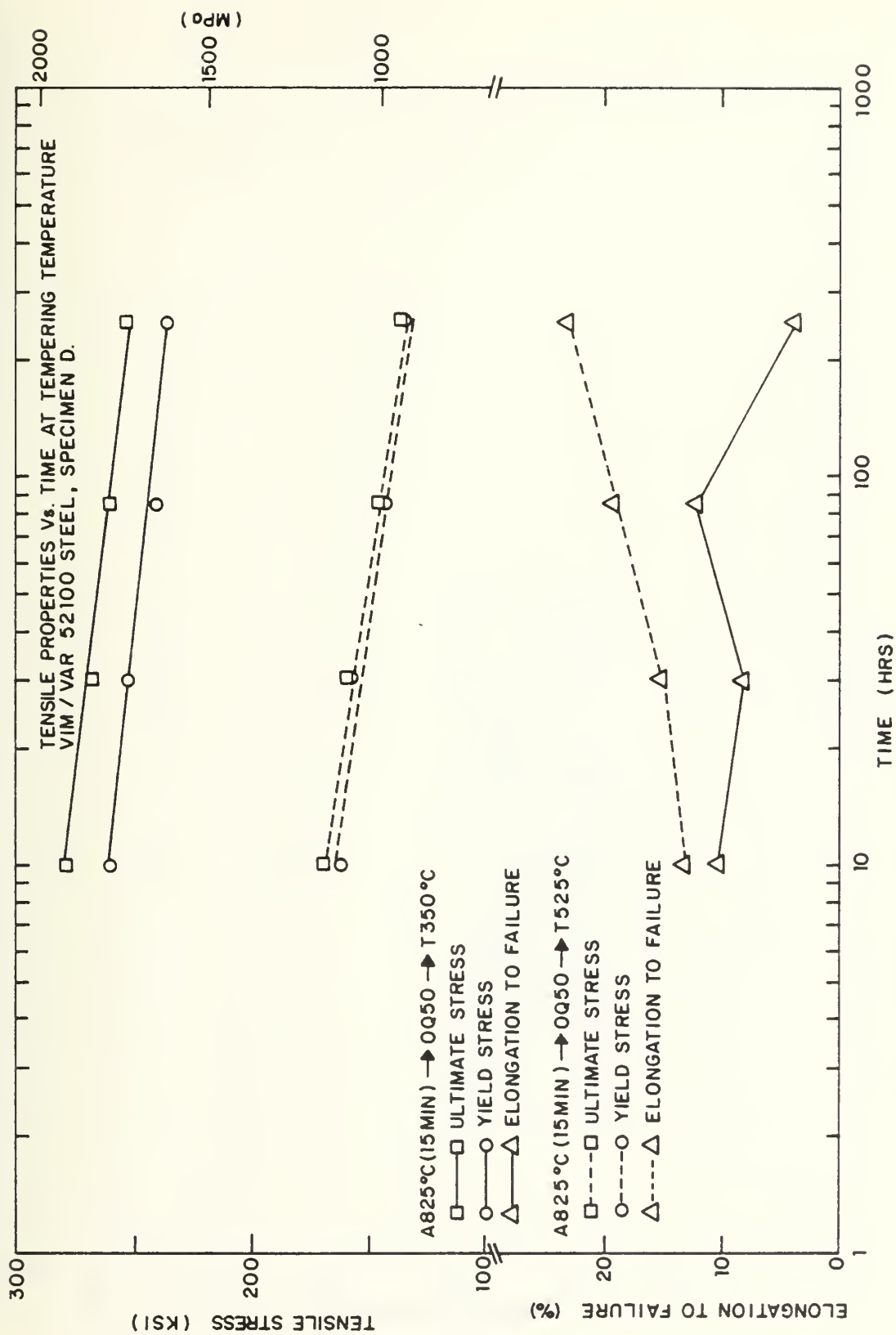


Figure 43. Tempering Response of Treatment-D (Tensile Strength).

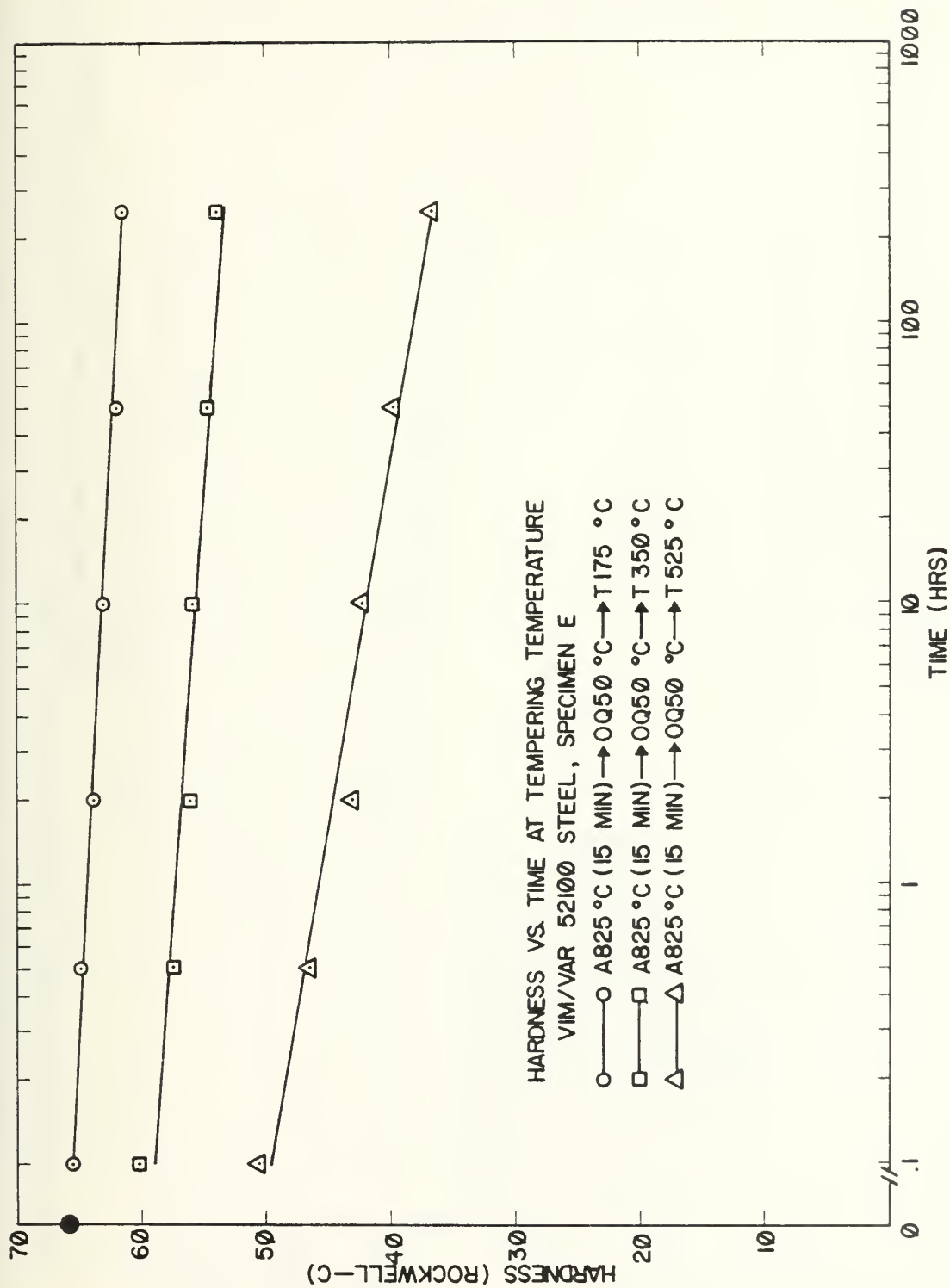


Figure 44. Tempering Response of Treatment-E (Hardness).

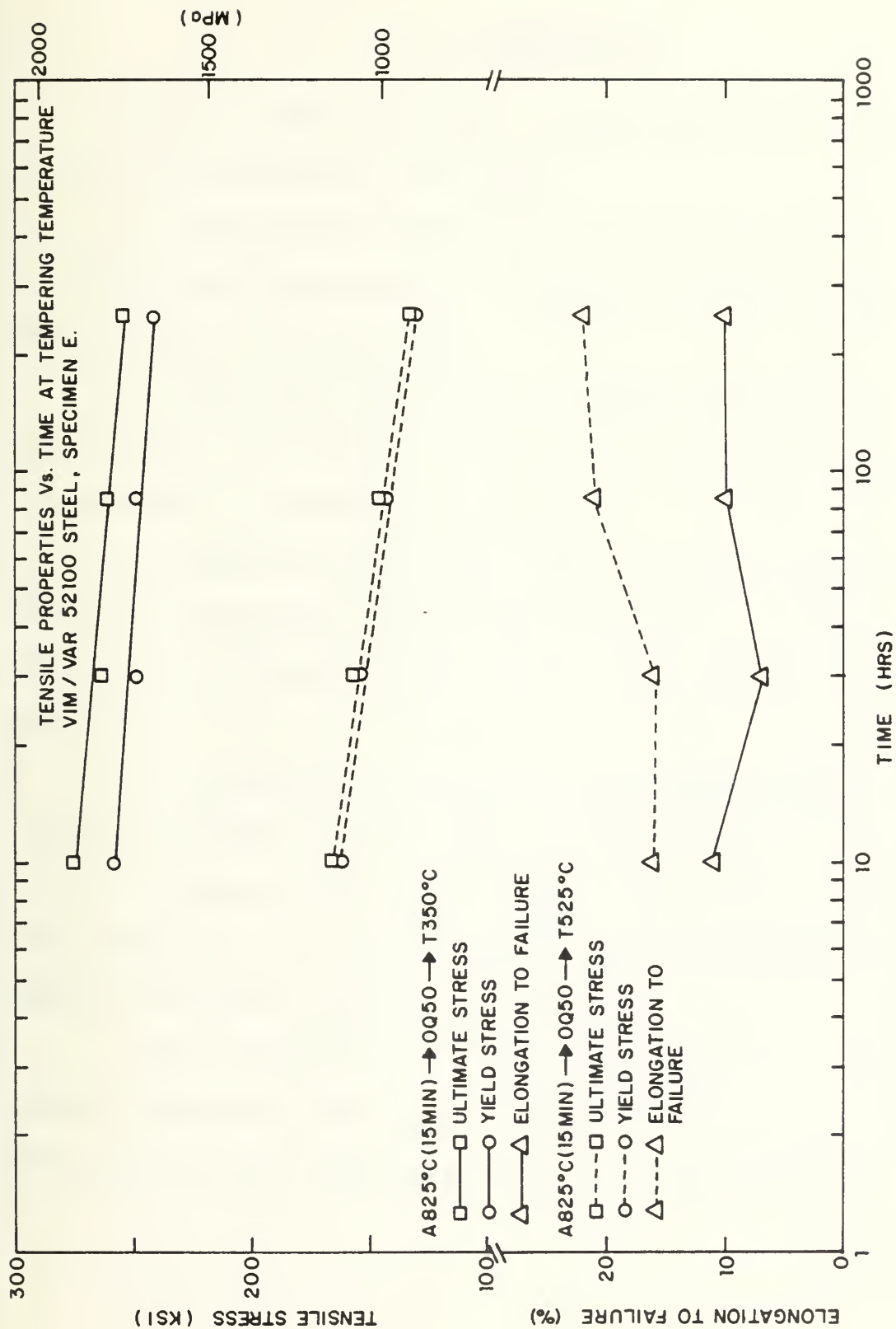


Figure 45. Tempering Response of Treatment-E (Tensile Strength).

IV. CONCLUSIONS

Based on the experimental observations and results, the following conclusions were drawn:

1. The thermo-mechanical treatments proposed and examined in this work significantly refined the microstructure of the as treated AISI 52100 steel.
2. The grain structure and carbide dispersion are more uniform when the starting structure is martensitic or a combination of martensite and bainite.
3. Pre-deformation heat treatments utilizing a 1000 degree Celsius (1830 degree F) are more effective in reducing the size of the residual carbide particles in the as-treated condition.
4. The hardening response of the thermo-mechanically treated material is more rapid and hardening can be accomplished at lower austenitizing temperatures than currently utilized. The quantity of retained austenite in the hardened condition is, however, somewhat higher.
5. The degradation of mechanical strength (hardness and tensile strength) with time at austenitizing temperature is decreased for the thermo-mechanically treated material.

LIST OF REFERENCES

1. Sherby, O.D., Walser, B., Young, C.M., and Cady, E.M., "Superplastic Ultra-High Carbon Steels," Scripta Met. v. 9, p. 569, 1975.
2. Goesling, W. H., Ballistic Characterization of Ultra-Carbon Steel, M.S. Thesis, Naval Postgraduate School, Monterey, CA, 1977.
3. Rowe, D. and Hamilton, D.R., The Microstructural, Mechanical, and Ballistic Characterization of Ultra-High Carbon Steel, M.S. Thesis, Naval Postgraduate School, Monterey, CA, 1977.
4. Sherby, O.D. "Superplasticity," Science Journal, v. 5, p. 75, 1969.
5. Hertzberg, R.W., Deformation and Fracture Mechanics of Engineering Materials, Wiley, pp. 152-155, 1976.
6. Ovama, T., Wadsworth, J., Korchynsky, M., and Sherby, O. D., Fifth International Conference on the Strength of Metals and Alloys, Conference Proceedings, Aachen, Germany, Perfamon Press, pp. 381-386, 1979.
7. Chung, I.S., The Influence of Thermomechanical Processing and Heat Treatment on the Fatigue Resistance and Fractographic Characteristics of a High-Carbon Bearing Steel, M.S. Thesis, Naval Postgraduate School, Monterey, CA, 1979.
8. Second Annual Report to Advanced Projects Research Agency Under Grant DAHC-15-73-G15, Superplastic Ultra-High Carbon Steels, Stanford University Press, by O.D. Sherby and B. Walsner, 1975.
9. Sherby, O.D., Superplasticity of Metals and Alloys, paper presented at Advanced Research Projects Agency Workshop, La Jolla, CA 1976.
10. Sherby, O.D., Harrigan, M.J., Chamagne, L., and Sauve, C., "Development of Fine Spheroidized Structures by Warm Rolling of High Carbon Steels," Transactions of the ASM, v. 62, p. 575, 1969.

11. McCauley, J.F., The Influence of Prior Warm Rolling on Fracture Toughness of Heat Treated AISI 52100 Steel, M.S. Thesis, Naval Postgraduate School, Monterey, CA, 1980.
12. Reed-Hill, R.E., Physical Metallurgy Principles, 2d ed., pp. 284-302, Van Nostrand, 1973.
13. Eschmann, P., Hasbargen, L., and Weignad, R., Ball and Roller Bearing, Heyden, 1958.
14. Krauss, G., Principles of Heat Treatment of Steel, American Society for Metals, 1978.
15. Metals Handbook, 9th Ed., v. 1, American Society for Metals, 1978.
16. Brooks, C.R., Heat Treatment of Ferrous Alloys, pp. 159-180, McGraw-Hill, 1979.
17. Siebert, C.A., Doane, D.V., and Breen, D.H., The Hardenability of Steels, pp. 65-138, American Society for Metals, 1977.
18. Grange, R.A. "Rapid Heat Treatment of Steel," Met. Trans. v. 2, pp. 65-78, 1971.
19. Monma, K., Maruta, R., Yamamoto, T., and Wakikado, Y., Jap. Inst. Metals J. V. 32, pp. 1198-1204, 1968.
20. Vincent, L. Coquillont, B., and Guiraldenq, P., "Fatigue Damage of Ball Bearing Steel: Influence of Phases Dispersed in a Martensitic Matrix," Met. Trans. v. 11A, pp. 1001-1006, 1980.
21. Stickels, C.A., "Carbide Refining Heat Treatments for 52100 Bearing Steel," Met. Trans., v. 5, pp. 865-874, 1974.
22. Parker, R.J., Zaretsky, E.V., Dietrich, M.W., Rolling Element Fatigue Lives of Four M-Series Steels and AISI 52100 at 150°F, NASA Technical Note D-7033, 1971.
23. ASTM A370-74, "Mech. Testing of Steel Products," 1974.
24. Ogilvie, R.E., "Retained Austenite by X-Ray," Norelco Reporter, 5(1959), p. 60.
25. Doig, A., Private Communication, 1980.

26. Samuels, L.E., Optical Microscopy of Carbon Steels, American Society for Metals, pp. 247-409, 1980.
27. Maurer, R., Private Communication, 1980.
28. Kar, R.J. Horn, R.M., and Zackay, V.F., "The Effect of Heat Treatment on Microstructure and Mechanical Properties of 52100 Steel," Met. Trans., v. 10A, pp. 1711-1717, 1979.

INITIAL DISTRIBUTION LIST

	No. Copies
1. Defense Technical Information Center Cameron Station Alexandria, Virginia 22314	2
2. Library, Code 0142 Naval Postgraduate School Monterey, California 93940	2
3. Department Chairman, Code 69Mx Department of Mechanical Engineering Naval Postgraduate School Monterey, California 93940	1
4. Assoc. Professor Terry R. McNelley, Code 69Mc Department of Mechanical Engineering Naval Postgraduate School Monterey, California 93940	4
5. Adj. Professor Donald H. Boone, Code 69B1 Department of Mechanical Engineering Naval Postgraduate School Monterey, California 93940	2
6. Dr. Michael R. Edwards Metallurgy Branch The Royal Military College of Science Shrivenham, Swindon, Wilts SN6-8LA England	3
7. Professor John P. Stark Department of Mechanical Engineering University of Texas Austin, Texas 78712	1
8. Professor George Krauss Department of Metallurgical Engineering Colorado School of Mines Golden, Colorado 80401	1
9. Assoc. Professor A.J. Perkins, Code 69Ps Department of Mechanical Engineering Naval Postgraduate School Monterey, California 93940	1

10. LT Clarence W. Schultz, USN
SUPSHIPS New Orleans
Code 205
Building 16
Naval Support Activity
New Orleans, LA 70142

4

Thesis

S3643

Schultz

193959

c.1

Effect of thermo-
mechanical treatment
on the microstructure
and mechanical prop-
erties of AISI 52100
steel.

Thesis

S3643

Schultz

193959

c.1

Effect of thermo-
mechanical treatment
on the microstructure
and mechanical prop-
erties of AISI 52100
steel.

thesS3643

Effect of thermomechanical treatment on



3 2768 002 00056 4

DUDLEY KNOX LIBRARY